X 62 64748

DE [redacted] D

DECLASSIFIED

Copy 368
RM L58C25

NACA RM L58C25

NACA

RESEARCH MEMORANDUM

INVESTIGATION OF AERODYNAMIC CHARACTERISTICS OF AN AIRPLANE CONFIGURATION HAVING TAIL SURFACES OUTBOARD OF THE WING TIPS AT MACH NUMBERS OF 2.30, 2.97, AND 3.51

By James D. Church, William C. Hayes, Jr.,
and William C. Sleeman, Jr.

Langley Aeronautical Laboratory
Langley Field, Va.

NATIONAL ADVISORY COMMITTEE
FOR AERONAUTICS

WASHINGTON

June 23, 1958

NATIONAL ADVISORY COMMITTEE FOR AERONAUTICS

RESEARCH MEMORANDUM

INVESTIGATION OF AERODYNAMIC CHARACTERISTICS OF AN AIRPLANE CONFIGURATION HAVING TAIL SURFACES OUTBOARD OF THE WING TIPS AT MACH NUMBERS OF 2.30, 2.97, AND 3.51

By James D. Church, William C. Hayes, Jr., and William C. Sleeman, Jr.

SUMMARY

An investigation has been conducted at the Langley Unitary Plan wind tunnel to determine the drag, static longitudinal and lateral stability, and longitudinal trim characteristics of an airplane configuration having tail surfaces outboard of the wing tips. Data were obtained at Mach numbers of 2.30, 2.97, and 3.51 at a Reynolds number of 2.03×10^6. Included in the basic data are some effects of Reynolds number, engine pack, and wing twist combined with toe-out of the vertical tails. Values of maximum lift-drag ratio at a Mach number of 2.97 for the model with the engine pack installed were about 5.85 and 5.60 for stabilizer deflections of -0.1° and -4.9°, respectively. These values would correspond to trim conditions for low-lift static margins of approximately 10 and 22 percent of the mean aerodynamic chord, respectively. With the 10 percent static margin (stabilizer deflection of -0.1°), however, longitudinal instability occurred above a lift coefficient of about 0.20. Positive directional stability of the model was practically invariant with angle of attack to 12°.

INTRODUCTION

Recent experimental and analytical studies (refs. 1 and 2) have indicated that airplane configurations employing horizontal tail surfaces outboard and rearward of the wing tips should result in an improvement in performance characteristics over conventional designs. Since this geometry logically results in twin vertical tails, these performance gains might be achieved while retaining adequate directional stability. Consequently, as part of a program by the National Advisory Committee for Aeronautics to investigate various configurations with high lift-drag ratio designed for sustained operation near $M = 3.0$, tests were conducted in the Langley Unitary Plan wind tunnel to determine the drag, static stability, and longitudinal trim characteristics of an outboard-tail model. Results from an investigation of a configuration representing a different approach to the general problem of attaining high lift-drag ratios are reported in reference 3.

Data for the present tests were obtained at Mach numbers of 2.30, 2.97, and 3.51 for angles of attack from -4° to 16° and for angles of sideslip of 4° and -4°. Included in the basic data are some effects of Reynolds number, engine pack, horizontal stabilizer, and wing twist combined with toe-out of the vertical tails. These data are presented without analysis.

SYMBOLS

The forces and moments are reduced to coefficient form and are referenced to the following axis systems: The lateral components are presented about the body axes shown in figure 1(a) and the longitudinal components are oriented with respect to the stability axes illustrated in figure 1(b). Moment coefficients are taken about an assumed center of gravity located at 65 percent of the mean aerodynamic chord of the wing alone (excluding the tails).

b — span of wing plus horizontal tails, 24.00 in.

C_L — lift coefficient, $\frac{\text{Lift}}{qS}$

$C_{D,c}$ — balance-chamber drag coefficient

$C_{D,b}$ — engine-pack base-pressure drag coefficient

$C_{D,d}$ — engine boundary-layer-diverter pressure-drag coefficient

$C_{D,i}$ — engine-pack internal-flow drag coefficient

C_D — external drag coefficient, $\frac{\text{Total drag}}{qS} - C_{D,c} - C_{D,b} - C_{D,i}$

C_m — pitching-moment coefficient, $\frac{\text{Pitching moment}}{qS\bar{c}}$

C_l rolling-moment coefficient, $\frac{\text{Rolling moment}}{qSb}$

C_n yawing-moment coefficient, $\frac{\text{Yawing moment}}{qSb}$

C_Y side-force coefficient, $\frac{\text{Side force}}{qS}$

$C_{m_{C_L}}$ longitudinal-stability parameter, $\frac{\partial C_m}{\partial C_L}$

$C_{m_{i_t}}$ stabilizer effectiveness parameter, $\left(\frac{\Delta C_m}{\Delta i_t}\right)_{C_L=0}$

C_{l_β} effective-dihedral parameter, $\left(\frac{\Delta C_l}{\Delta \beta}\right)_{\beta=\pm 4^\circ}$

C_{n_β} directional-stability parameter, $\left(\frac{\Delta C_n}{\Delta \beta}\right)_{\beta=\pm 4^\circ}$

C_{Y_β} side-force parameter, $\left(\frac{\Delta C_Y}{\Delta \beta}\right)_{\beta=\pm 4^\circ}$

$\bar{c}$ mean aerodynamic chord of wing plus horizontal tails, 12.95 in.

i_t horizontal-tail incidence angle relative to center line of the bodies attached to the wing tips (positive when trailing edge is down), deg

L/D lift-drag ratio

M free-stream Mach number

p_t free-stream stagnation pressure, lb/sq ft abs

q free-stream dynamic pressure, lb/sq ft

R Reynolds number based on $\bar{c}$

S area of wing plus horizontal tails including wing-body intercept (wing-tip and tail-root chords are assumed to lie on the center line of the bodies attached to the wing tips), 1.7391 sq ft

[redacted]

α angle of attack referred to fuselage reference line, deg

β angle of sideslip referred to fuselage center line, deg

δ_v vertical-tail incidence relative to center line of the bodies attached to the wing tips (positive when trailing edge is to the left; $\pm$ denotes toe-out wherein both tails are deflected with trailing edge inboard), deg

θ_w wing twist of theoretical tip chord with respect to the root chord about the 50-percent-chord line (positive when trailing edge of tip chord is down), deg

Subscripts:

min minimum

max maximum

S stability

APPARATUS AND MODEL

The tests were conducted in the high Mach number test section of the Langley Unitary Plan wind tunnel. This tunnel is of the variable-pressure, continuous-flow type with a test section 4 feet square and approximately 7 feet in length. Mach number may be varied continuously from about 2.3 to 4.8 by means of an asymmetric sliding-block nozzle.

Sketches of the model and its engine pack are presented in figure 2 and the geometric characteristics are given in table I. Photographs of the model are shown in figure 3. The cross section of the basic fuselage was semicircular from the nose rearward for about 22 inches, fairing smoothly from this point to a circular base. Mounted beneath the fuselage and extending to a point flush with the model base was a detachable engine pack. (See fig. 2(a).) This pack consisted of a two-dimensional split inlet ducted to exhaust through three choked nozzles. An integral part of the pack was the wedge-type boundary-layer diverter located on the upper surface of the inlet-duct housing.

The trapezoidal wing had 70° of sweep at the leading edge and was mounted with its theoretical root chord on the fuselage reference line. This surface had an aspect ratio of 1.0000, a taper ratio of 0.3919, a dihedral angle of -5.3°, and NACA 65A004 airfoil sections. Two different wings were tested on the model. One was twisted about the 0.50-chord line so that the incidence between the theoretical tip and root chords was -2.8°. The other wing was untwisted $(\theta_W = 0^\circ)$. A slender body was affixed to each wing tip and hence was inclined by the angle θ_W to the fuselage reference line. The profile of these bodies of revolution consisted of a short cylindrical section inserted between an ogival nose and tail.

The vertical and horizontal tails had trapezoidal plan forms and were swept back 60° at the leading edge. These surfaces were considered to be undeflected when alined with the center lines of the wing-tip bodies. All tail panels had an aspect ratio of 0.9185, taper ratio of 0.3069, 0° of dihedral, and NACA 65A003 airfoil sections.

Forces and moments for the model were measured by means of a six-component internal strain-gage balance. This balance was attached, by means of a sting, to the tunnel central support system. Included in the model support system was a remotely operated, adjustable angle coupling which permitted tests to be made at various angles of attack simultaneously with variations in the angle of sideslip.

TESTS

Tests were conducted for all configurations through an angle-of-attack range of approximately -4° to 16° at an angle of sideslip of 0°. Lateral-stability derivatives were determined from tests made through this angle-of-attack range for angles of sideslip of about 4° and -4°, with and without the engine pack, at $M = 2.97$. Tests to determine stabilizer effectiveness utilized incidence angles of -0.1° and -4.9°. All tests except those with the untwisted wing $(\theta_W = 0^\circ)$ were made with the vertical tails toed-out $(\delta_V = \pm 1.5^\circ)$.

Average Mach numbers, stagnation pressures, dynamic pressures, and Reynolds number are listed in the following table:

M	p_t, lb/sq ft abs	q, lb/sq ft	R (based on $\bar{c}$)
2.30	1,434	425	2.03×10^6
2.97	2,050	360	2.03
3.51	2,726	304	2.03

Stagnation temperature was maintained at 155° F for all Mach numbers.

Pressure measurements were recorded during one of the tests with the engine pack installed in order to obtain the drag increments associated with the engine-pack base pressure, internal flow, and boundary-layer diverter pressure. Data were also obtained at $M = 2.97$ on the untwisted-wing configuration without the engine pack and with all tail surfaces at a neutral setting in order to establish the effect of Reynolds number on minimum drag. This test was conducted near zero lift over a Reynolds number range of 0.51×10^6 to 6.4×10^6.

Transition was fixed on all configurations by means of roughness strips placed around the fuselage and wing-tip bodies about 2 inches behind the noses, and along the 10-percent-chord lines (upper and lower surfaces) of the wing and stabilizers. The strips were 1/32 inch wide and were formed by embedding No. 60 carborundum grains in a plastic adhesive. Two densities were employed: one test utilized about 150 grains per inch of strip (referred to as heavy) and all other configurations utilized about 50 grains per inch of strip (light).

CORRECTIONS AND ACCURACY

Tunnel pressure gradients in the region of the model have been found to be sufficiently small so as not to induce any measurable buoyancy effects on the model. Also, angularity surveys indicate negligible misalinement of the flow at the test Mach numbers. In addition, all angles of attack and sideslip have been corrected for deflection of the balance and sting due to load.

The balance-chamber drag (defined herein as the force that results from the balance-chamber pressure acting over the entire cross section of the base, including the sting) has been subtracted from the drag results for all configurations. The following additional forces have been subtracted from the drag results for the configurations with engine pack: base-pressure drag (pressure force acting over all of detachable-pack base area except for the three exits) and internal drag (force computed from duct and exit pressures by using standard momentum-balance equation).

Accuracy of the presented data based on balance and tunnel calibration is estimated to be within the following limits:

M	± 0.015
α, deg	± 0.2
β, deg	± 0.2
i_t, deg	± 0.1
δ_v, deg	± 0.1
θ_w, deg	± 0.1

[redacted]

C_L	±0.003
C_D	±0.0008
C_m	±0.003
C_l	±0.0005
C_n	±0.001
C_Y	±0.002

This table gives the accuracy of the absolute value of the quantities for use in evaluating the possible error in isolated data. Experience with repeatability of data indicates that probable errors can be considered to be roughly one-half as large as the values in the table.

PRESENTATION OF RESULTS

The basic results of the investigation are presented in figures 4 to 10 and some summary results are contained in figures 11 to 15. An abbreviated outline of figure content follows:

SUMMARY OF RESULTS

The main results of an investigation at Mach numbers of 2.30, 2.97, and 3.51 of an outboard-tail configuration at a Reynolds number of 2.03×10^6 are as follows:

Values of maximum lift-drag ratio $(L/D)_{max}$ at a Mach number of 2.97 for the model with the engine pack installed were about 5.85 and 5.60 for stabilizer deflections of -0.1° and -4.9°, respectively. These values would correspond to trim conditions for low-lift static margins of approximately 10 and 22 percent of the mean aerodynamic chord, respectively. With the 10 percent static margin (control deflection of -0.1°), however, longitudinal instability occurred above a lift coefficient of about 0.20. This instability was due to a stability loss of the wing-body combination and to an equal degree to the reduction in the stability contribution of the tail surfaces. Twisting the wing -2.8° (and consequently deflecting the horizontal stabilizer an equal amount) in conjunction with $\pm1.5^{\circ}$ toe-out of the vertical tails increased $(L/D)_{max}$ about 0.3 for the model without the engine pack at a Mach number of 2.97. An identical increase in this parameter resulted from the addition of the horizontal tails to the configuration with twisted wing and toed-out tails. In both instances this increase was due to a decrease in drag due to lift.

The directional stability $C_{n_{\beta}}$ of the model with engine pack was about 0.0015 and was practically invariant with angle of attack to 12°. The values of $C_{n_{\beta}}$ were reduced by a constant value of about 0.0005 by the addition of the engine pack to the model. The model with the engine pack had negative effective dihedral for angles of attack less than 4.5°.

Langley Aeronautical Laboratory,
National Advisory Committee for Aeronautics,
Langley Field, Va., March 14, 1958.

REFERENCES

1. Sleeman, William C., Jr.: Preliminary Study of Airplane Configurations Having Tail Surfaces Outboard of the Wing Tips. NACA RM L58B06, 1958.

2. Spearman, M. Leroy, and Robinson, Ross B.: Aerodynamic Characteristics of a Canard and an Outboard-Tail Airplane Model at a Mach Number of 2.01. NACA RM L58B07, 1958.

3. Kelly, Thomas C., Carmel, Melvin M., and Gregory, Donald T.: An Exploratory Investigation at Mach Numbers of 2.50 and 2.87 of a Canard Bomber-Type Configuration Designed for Supersonic Cruise Flight. NACA RM L58B28, 1958.

[redacted]

TABLE I.- GEOMETRIC CHARACTERISTICS OF MODEL

Wing plus horizontal tails (used in reduction of data):	
Area, sq ft	1.7391
Span, ft	2.000
Mean aerodynamic chord, ft	1.0790
Aspect ratio	2.3000
Taper ratio	0.1271
Wing:	
Area, sq ft	1.3611
Span, ft	1.1667
Mean aerodynamic chord, ft	1.2409
Aspect ratio	1.0000
Taper ratio	0.3919
Airfoil section	NACA 65A004
Twist, deg:	
Root	0
Tip	-2.8
Dihedral, deg	-5.3
Leading-edge sweepback, deg	70.0
Volume, cu ft	0.0295
Horizontal or vertical tail (panel geometry):	
Area, sq ft	0.1890
Span, ft	0.4167
Mean aerodynamic chord, ft	0.4962
Aspect ratio	0.9185
Taper ratio	0.3069
Airfoil section	NACA 65A003
Twist, deg	0
Dihedral, deg	0
Leading-edge sweepback, deg	60
Volume (exposed), cu ft	0.0013
Basic fuselage:	
Length, ft	2.8057
Fineness ratio	12.5
Volume, cu ft	0.0694
Wing-tip body:	
Length, ft	2.0833
Fineness ratio	16.6667
Volume, cu ft	0.0169
Engine pack:	
Base area (excluding the three exits), sq ft	0.0178
Enclosed volume, cu ft	0.0181

[redacted]

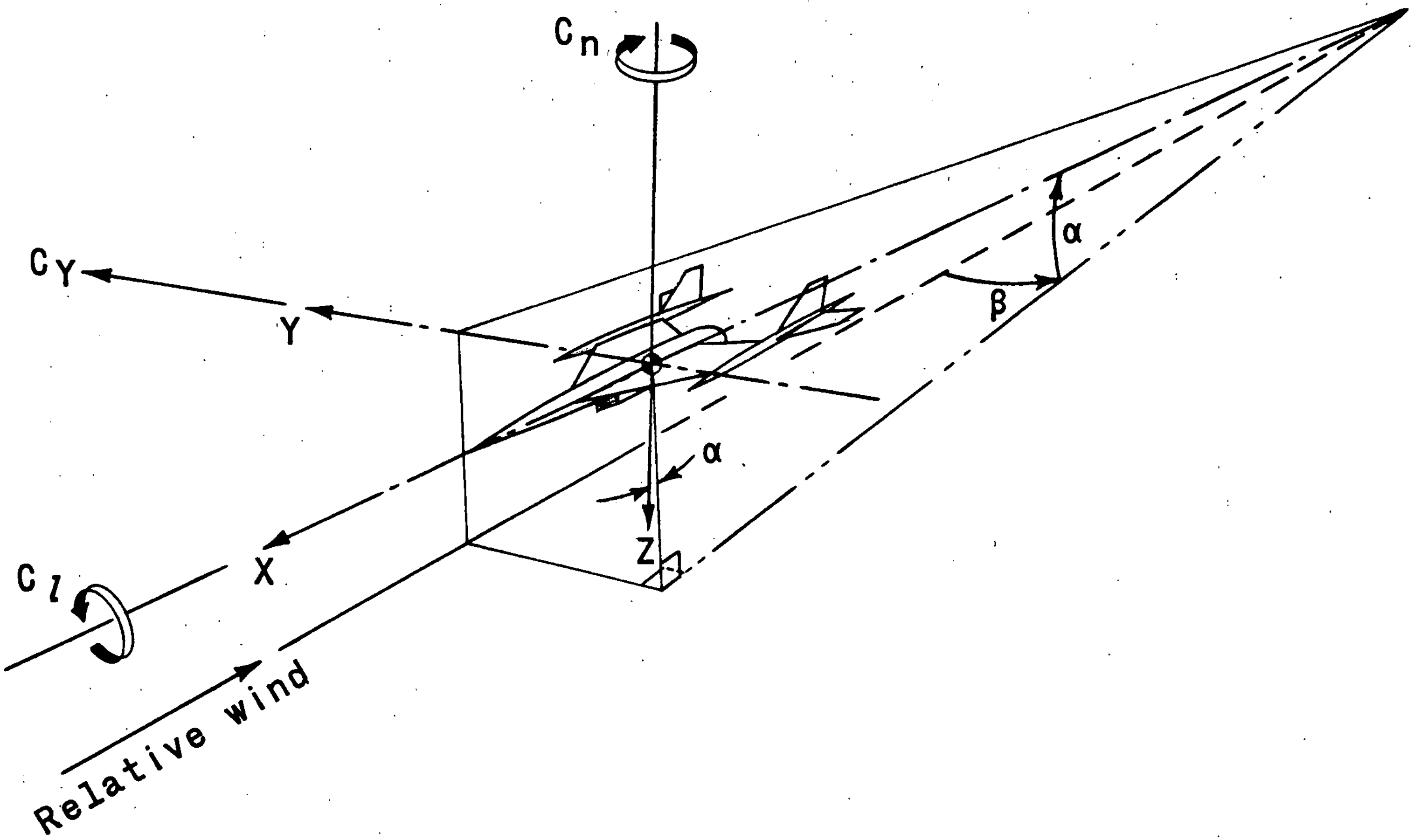

(a) Body axes.

Figure 1.- Systems of axes. Arrows indicate directions of positive forces, moments, and angles.

[redacted]

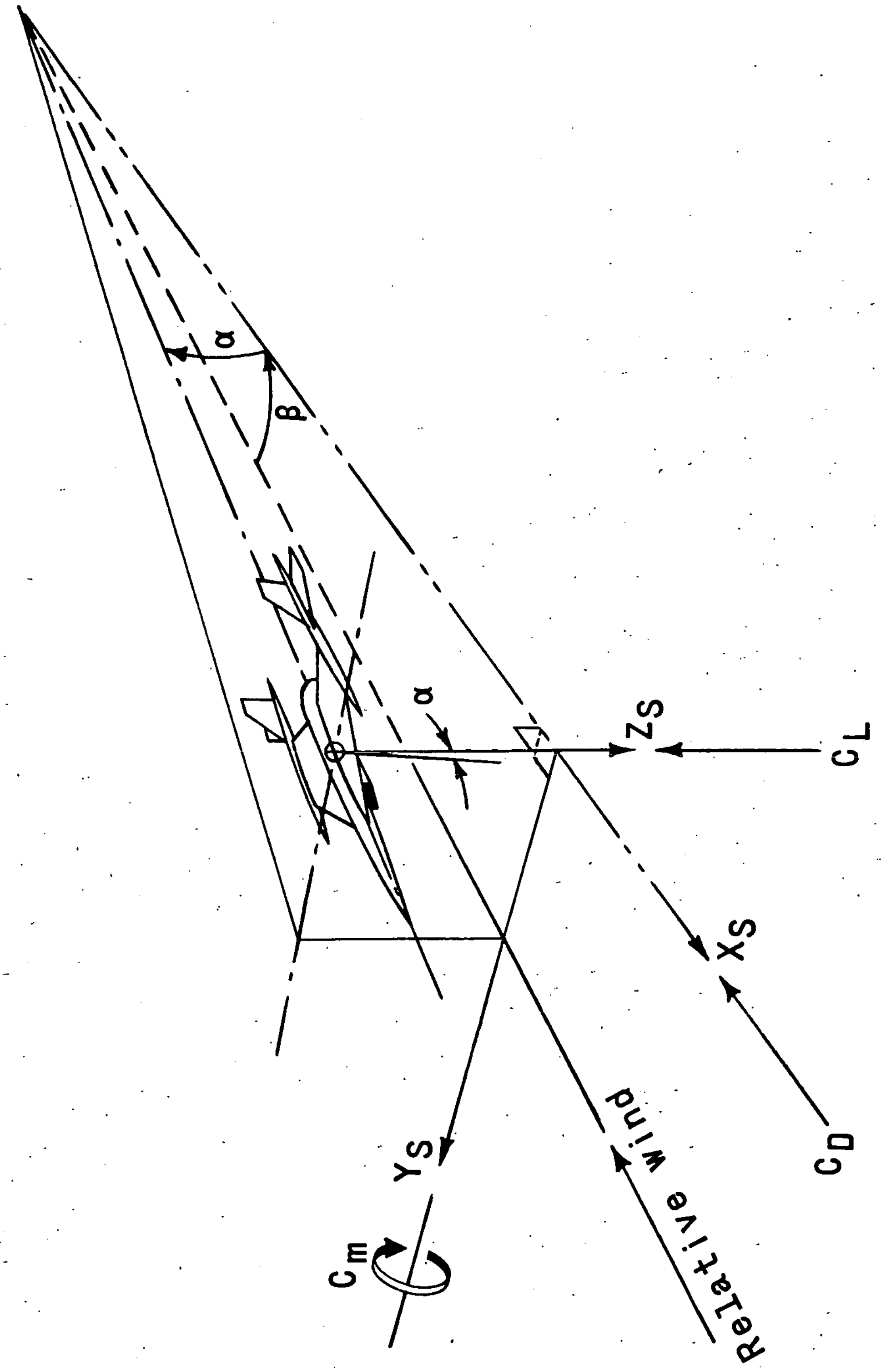

(b) Stability axes.

Figure 1.- Concluded.

[redacted]

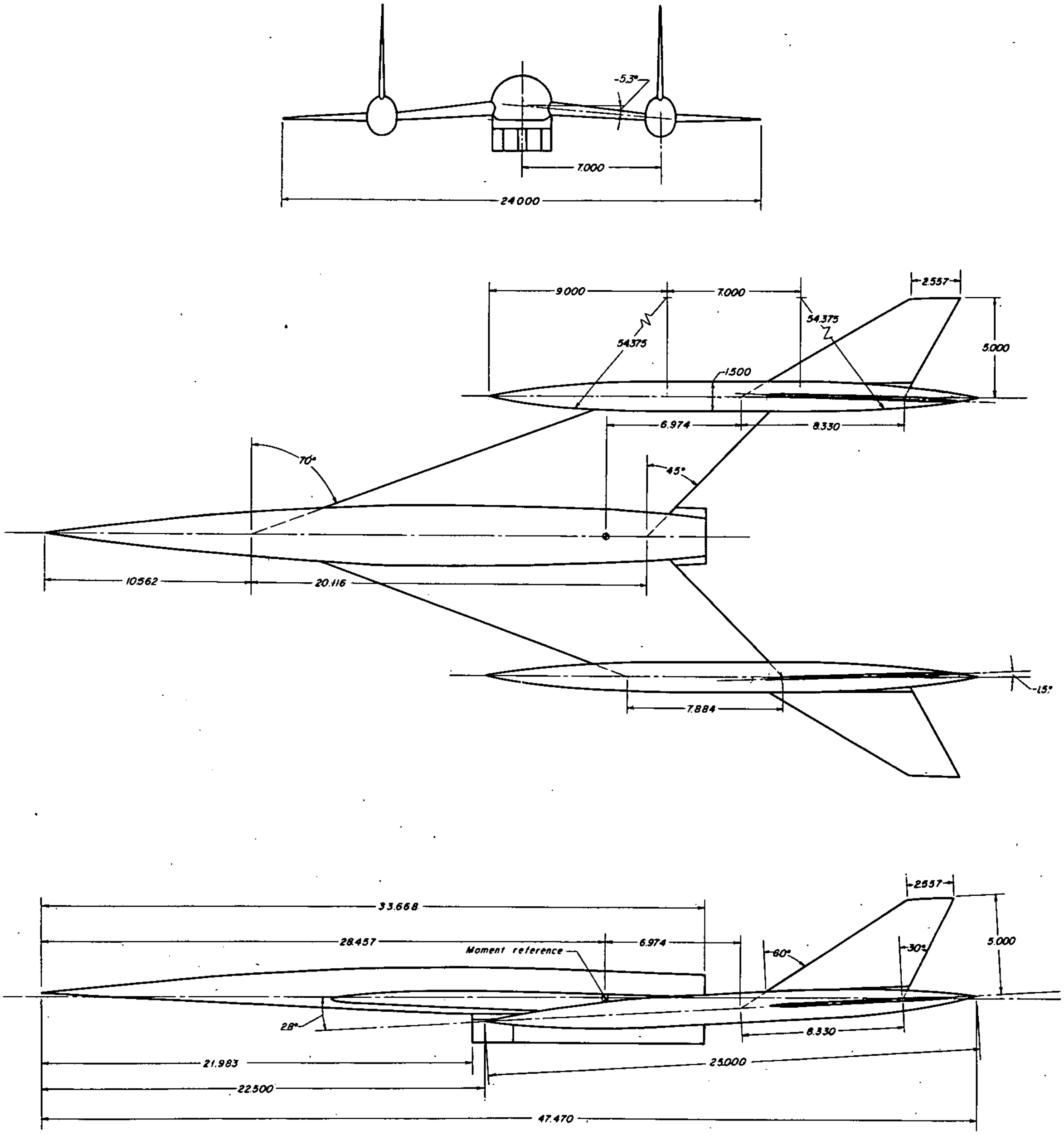

(a) Three-view drawing of model.

Figure 2.- General arrangement of outboard-tail model. All dimensions are in inches.

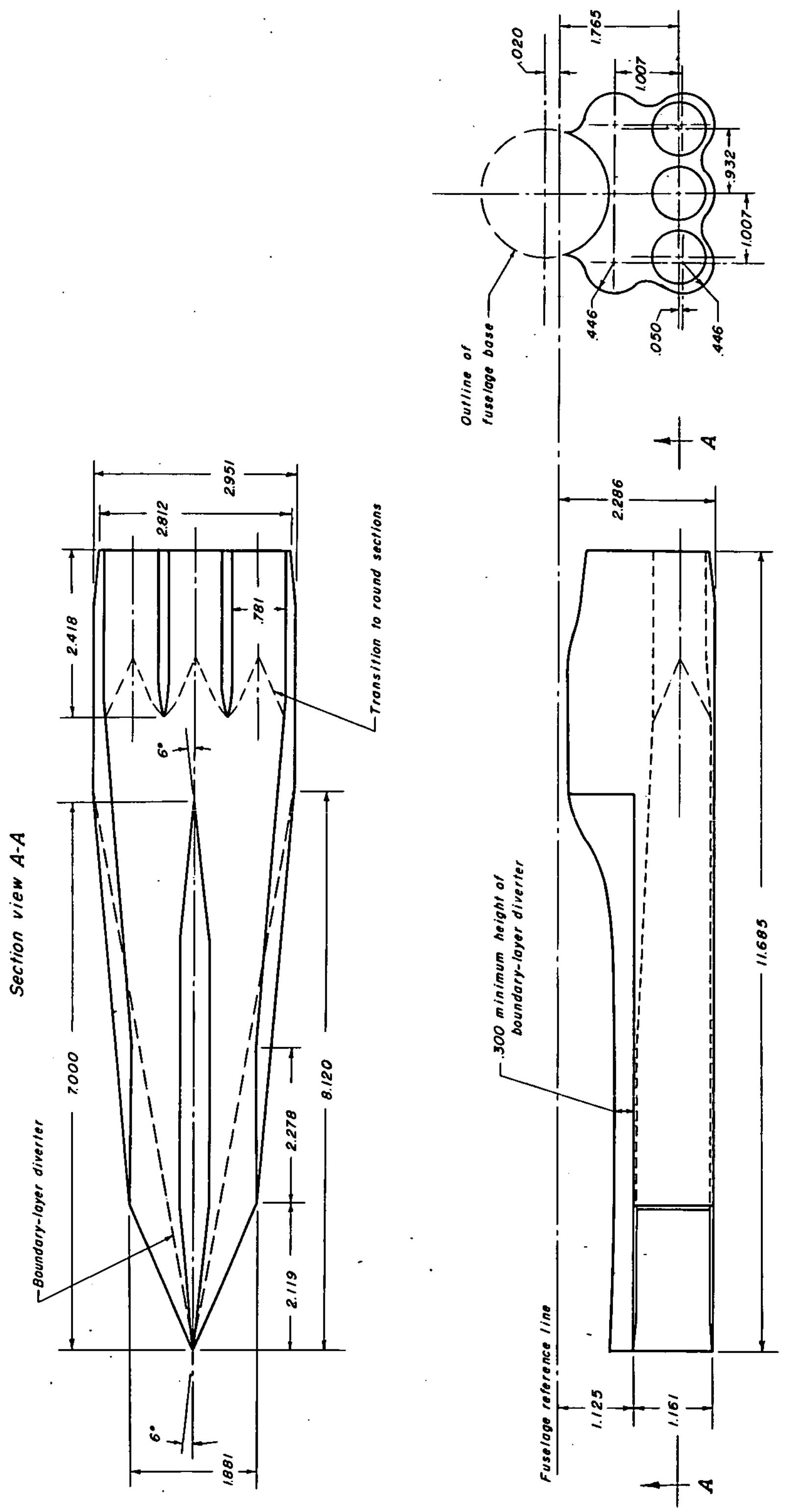

(b) Details of engine pack.

Figure 2.- Concluded.

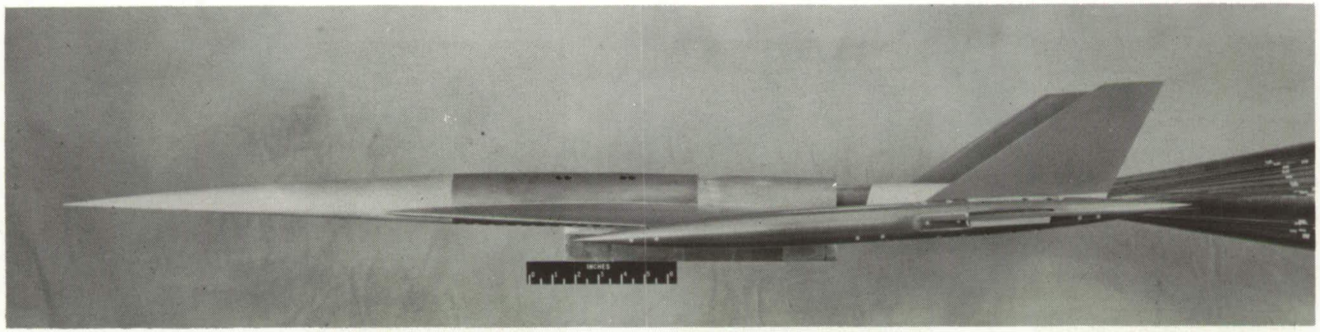

(a) Side view. L-57-4302

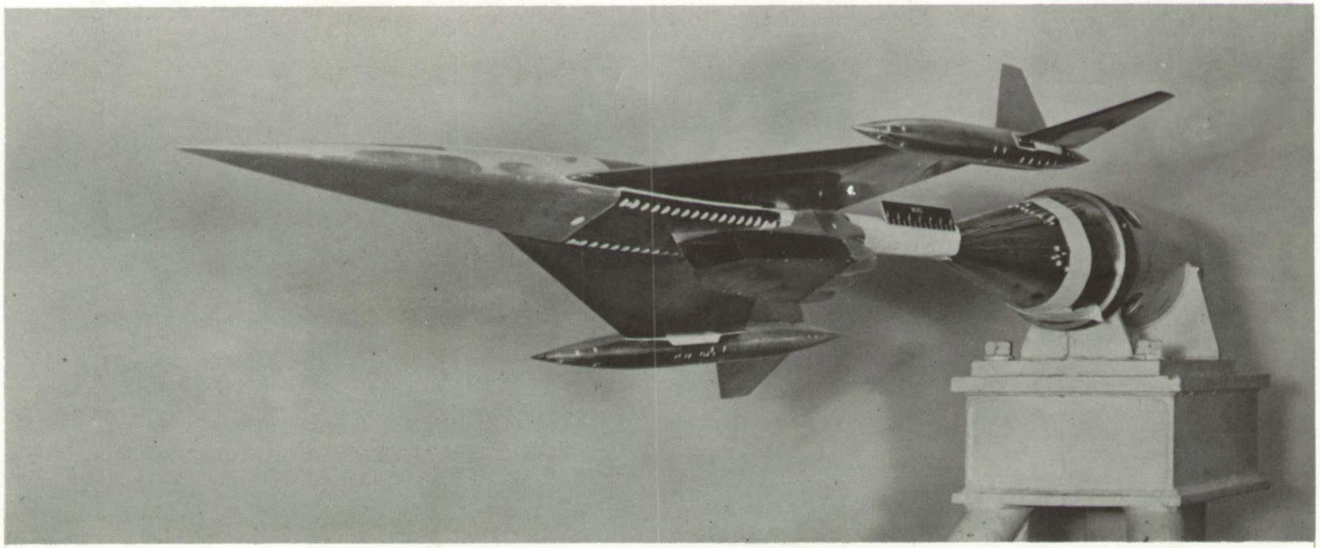

(b) Three-quarter front view. L-57-4301

Figure 3.- Photographs of model.

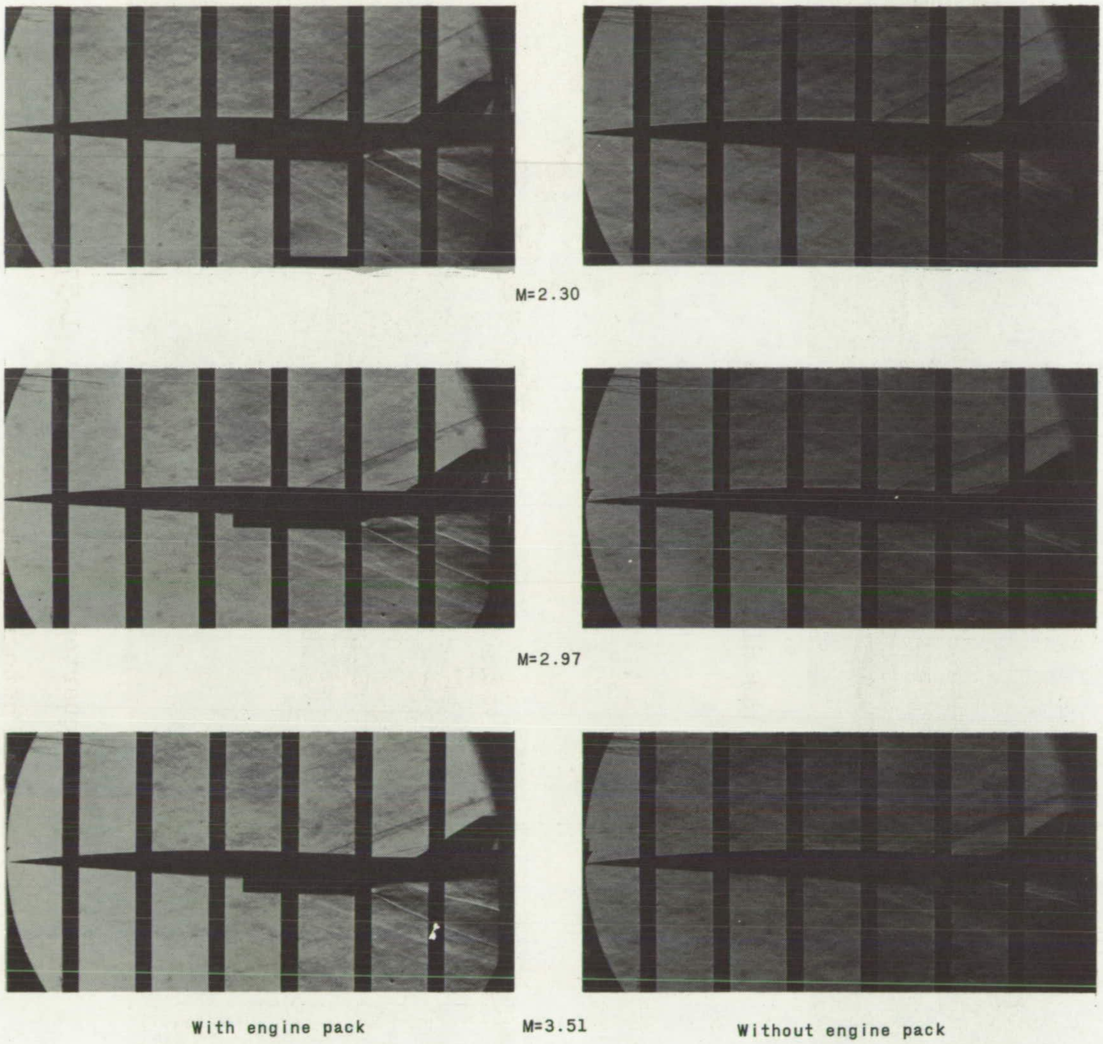

L-58-175

(a) $\alpha = 0^\circ$; $\theta_w = -2.8^\circ$; $\delta_v = \pm 1.5^\circ$; $i_t = -0.1^\circ$; $\beta = 0^\circ$.

Figure 4.- Typical schlieren photographs.

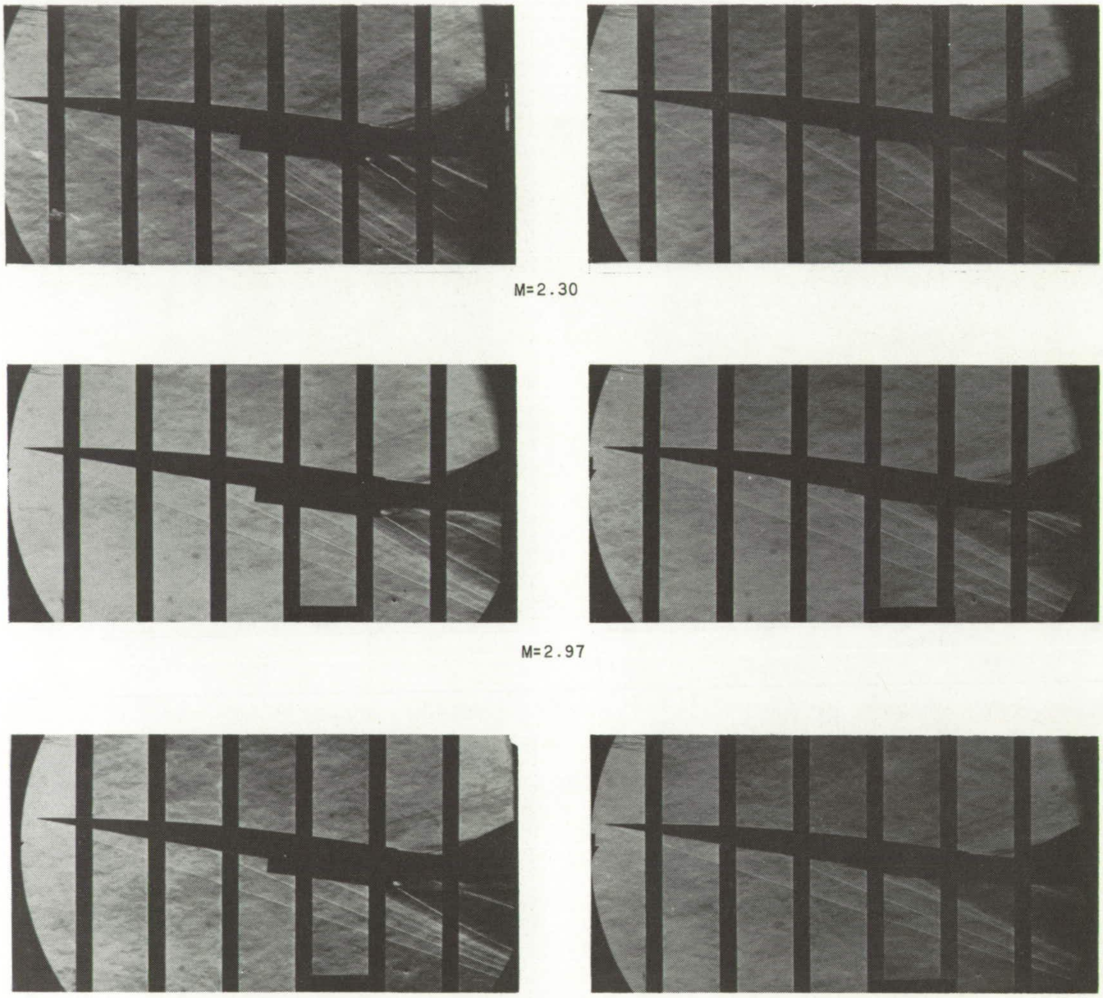

(b) $\alpha = 6.0^{\circ}$; $\theta_W = -2.8^{\circ}$; $\delta_V = \pm 1.5^{\circ}$; $i_t = -0.1^{\circ}$; $\beta = 0^{\circ}$. L-58-176

Figure 4.- Continued.

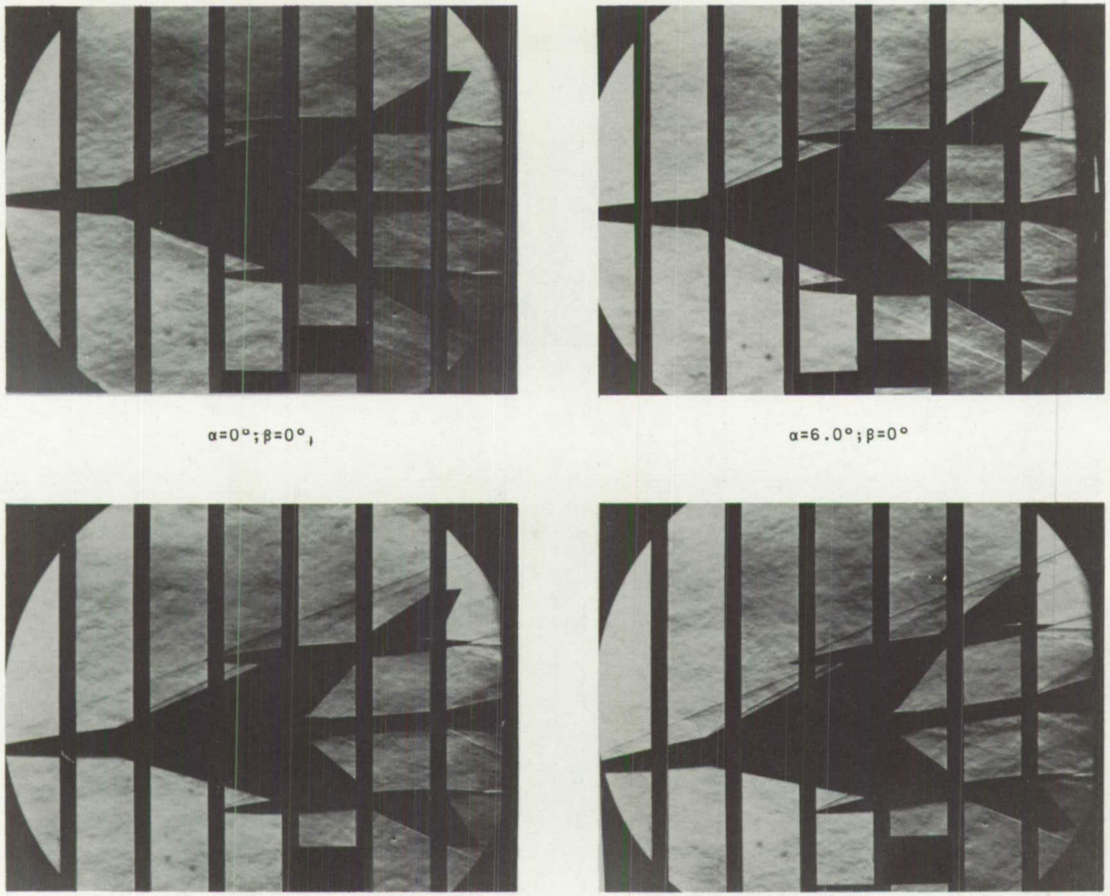

(c) Model without engine pack at $M = 2.97$; $\theta_w = 0^{\circ}$; $\delta_v = 0^{\circ}$; $i_t = -0.1^{\circ}$. L-58-177

Figure 4.- Concluded.

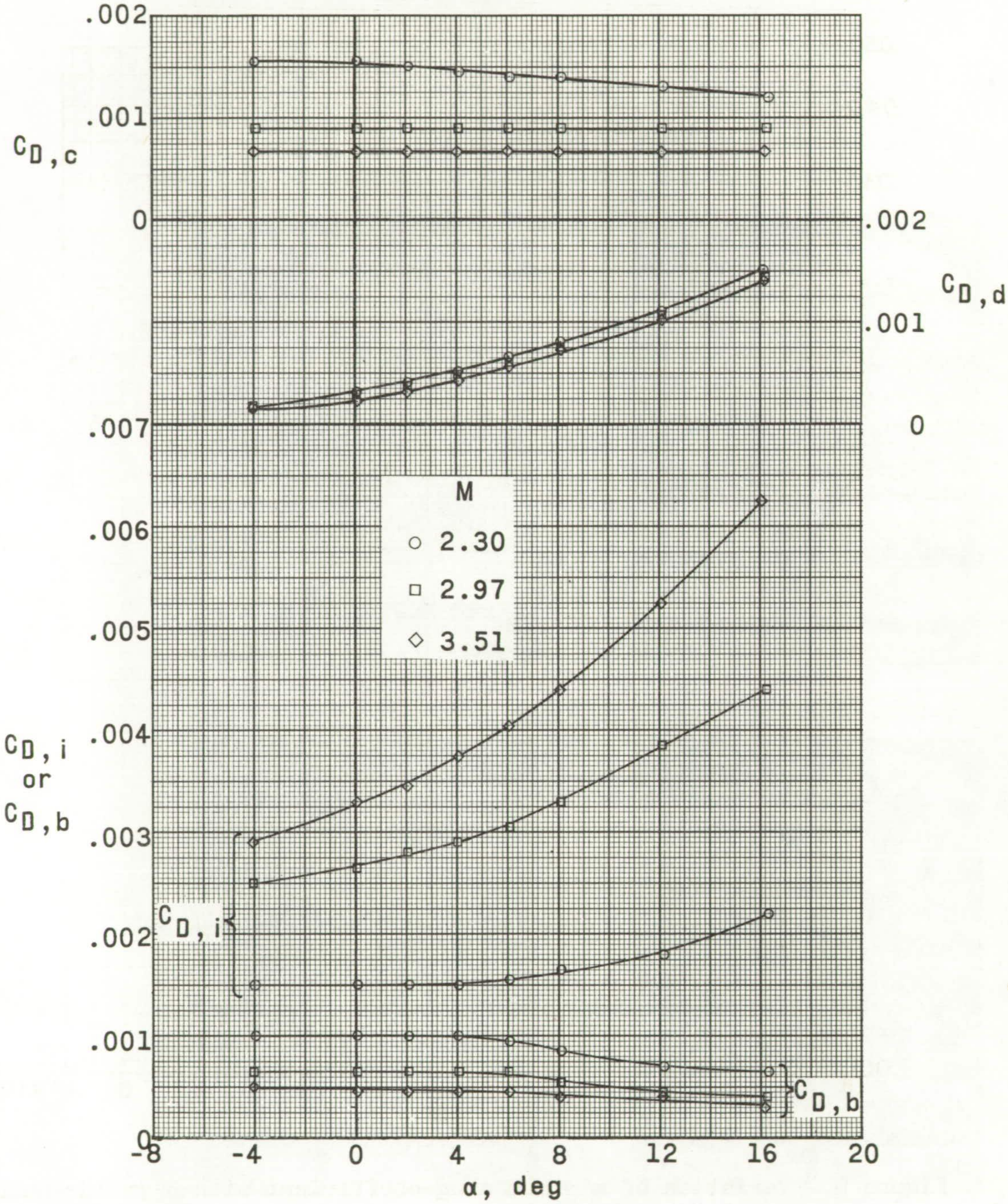

Figure 5.- Variation of balance-chamber, diverter-pressure, internal flow, and base-pressure drag coefficients with angle of attack. $\theta_w = -2.8^\circ$; $\delta_v = \pm1.5^\circ$; $i_t = -0.1^\circ$; $\beta = 0^\circ$.

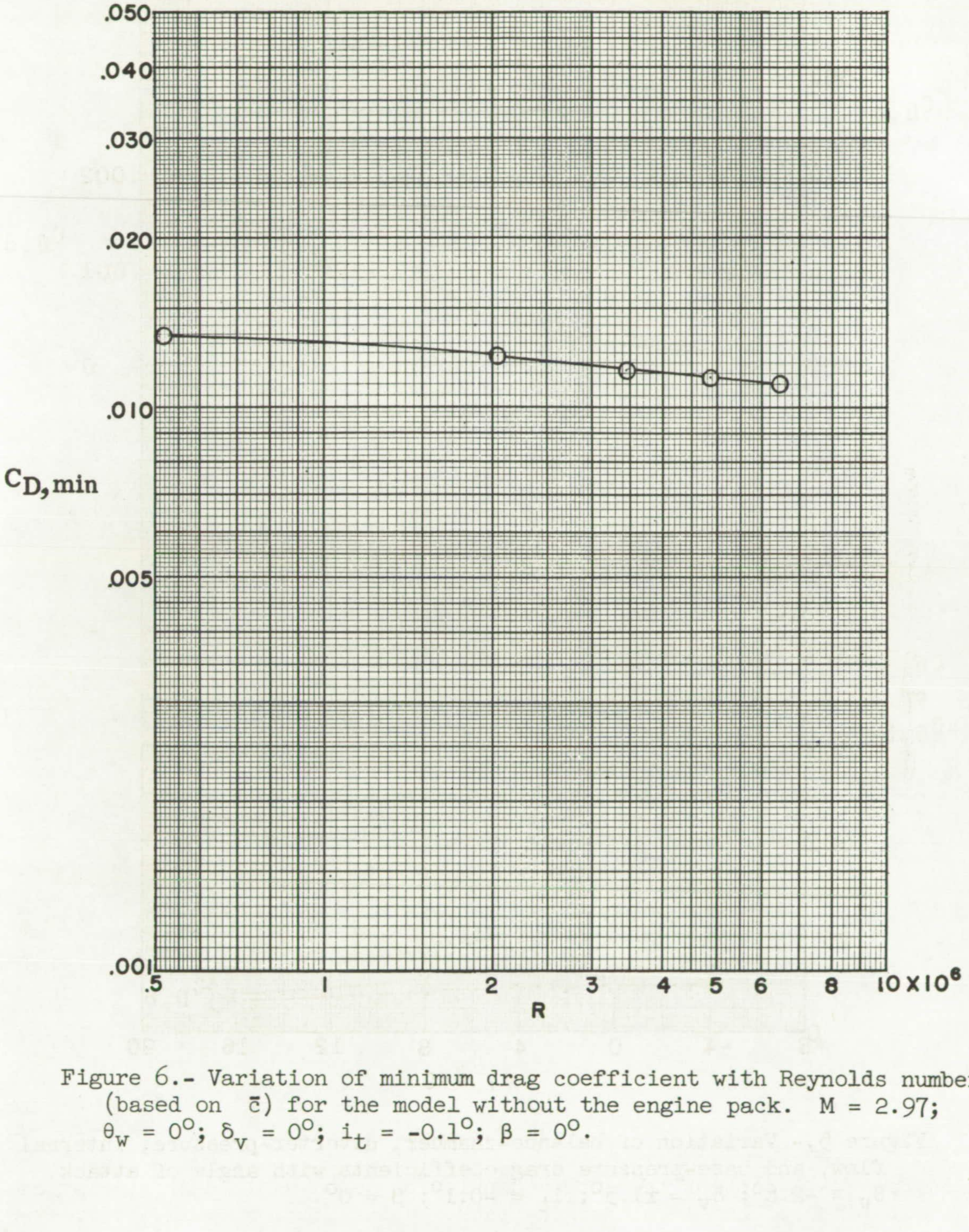

Figure 6.- Variation of minimum drag coefficient with Reynolds number (based on $\bar{c}$) for the model without the engine pack. M = 2.97; $\theta_w = 0^{\circ}$; $\delta_v = 0^{\circ}$; $i_t = -0.1^{\circ}$; $\beta = 0^{\circ}$.

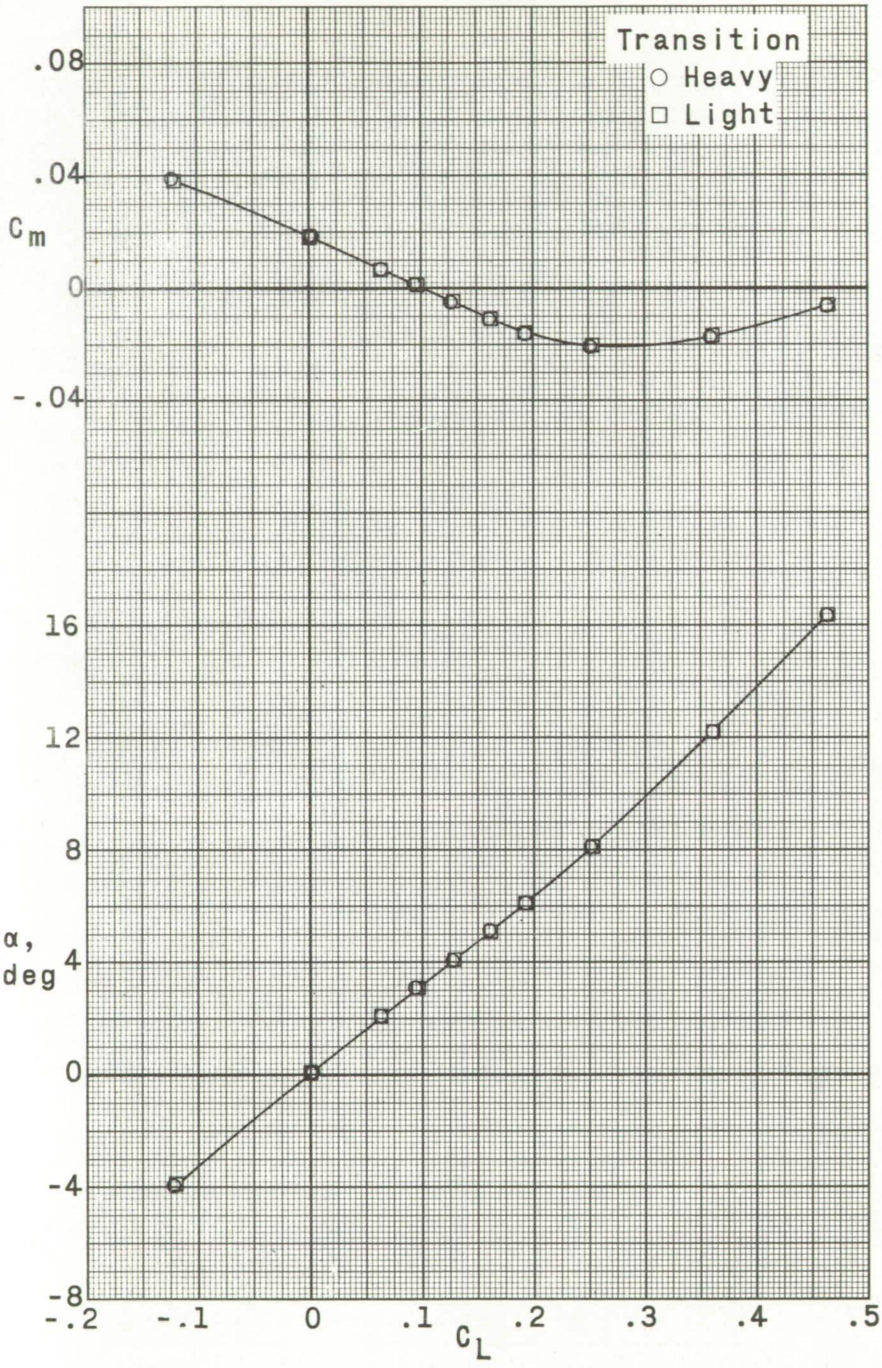

(a) M = 2.30.

Figure 7.- Effect of transition density on aerodynamic characteristics in pitch of model with engine pack. $\theta_w = -2.8^\circ$; $\delta_v = \pm 1.5^\circ$; $i_t = -0.1^\circ$; $\beta = 0^\circ$.

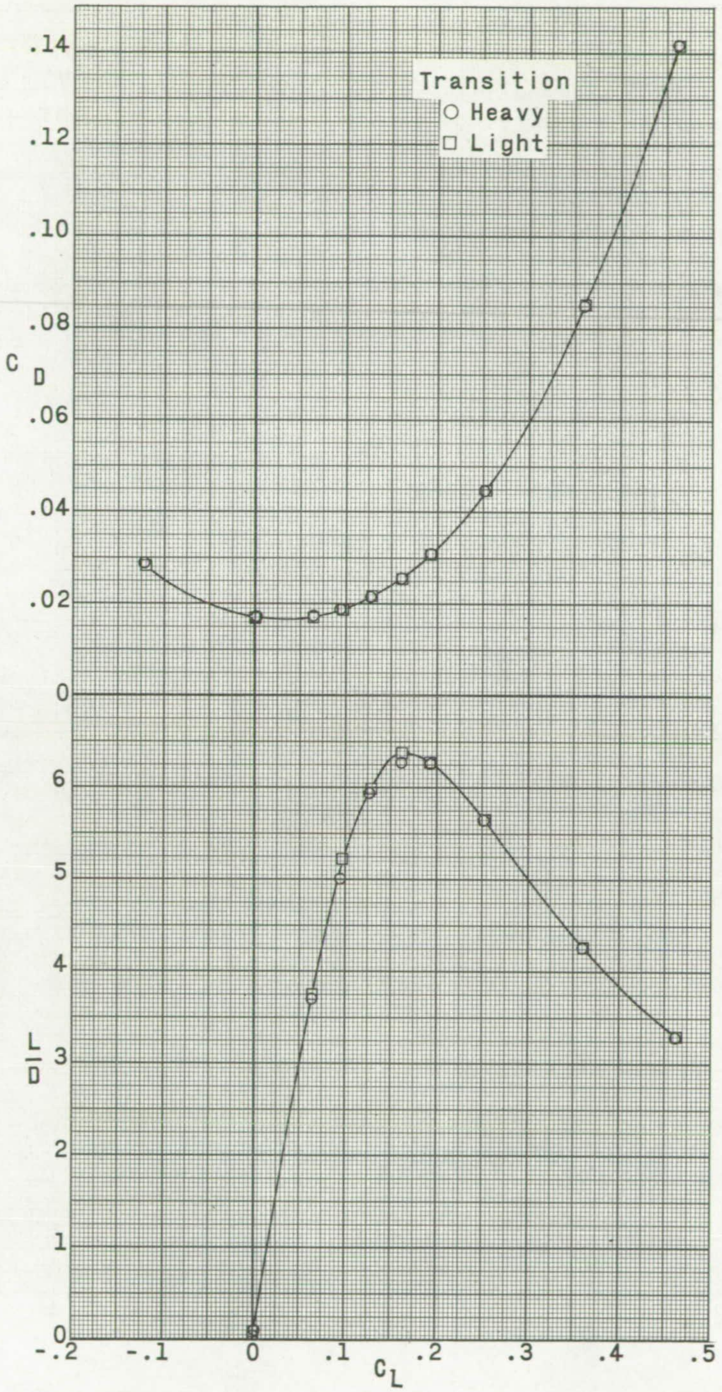

(a) Concluded.

Figure 7.- Continued.

[redacted]

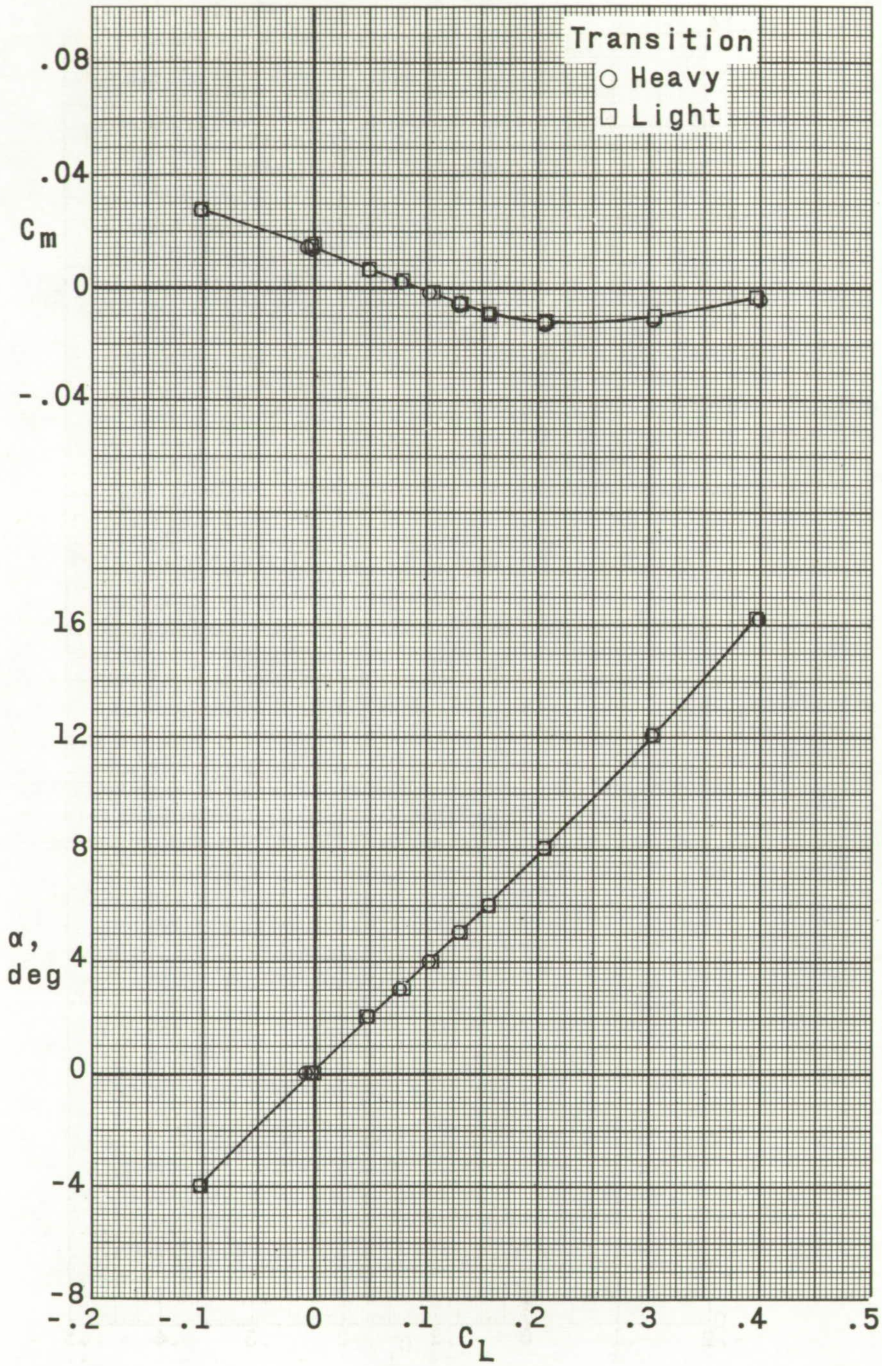

(b) M = 2.97.

Figure 7.- Continued.

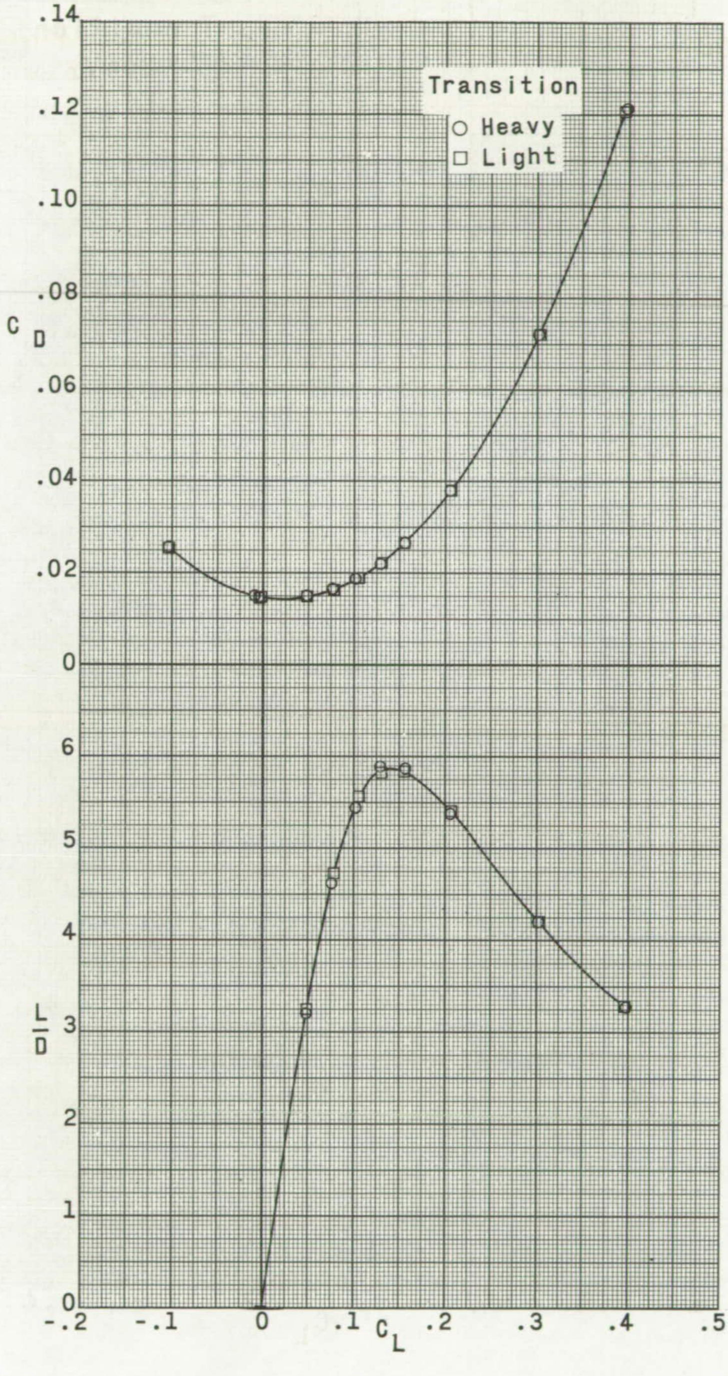

(b) Concluded.

Figure 7.- Continued.

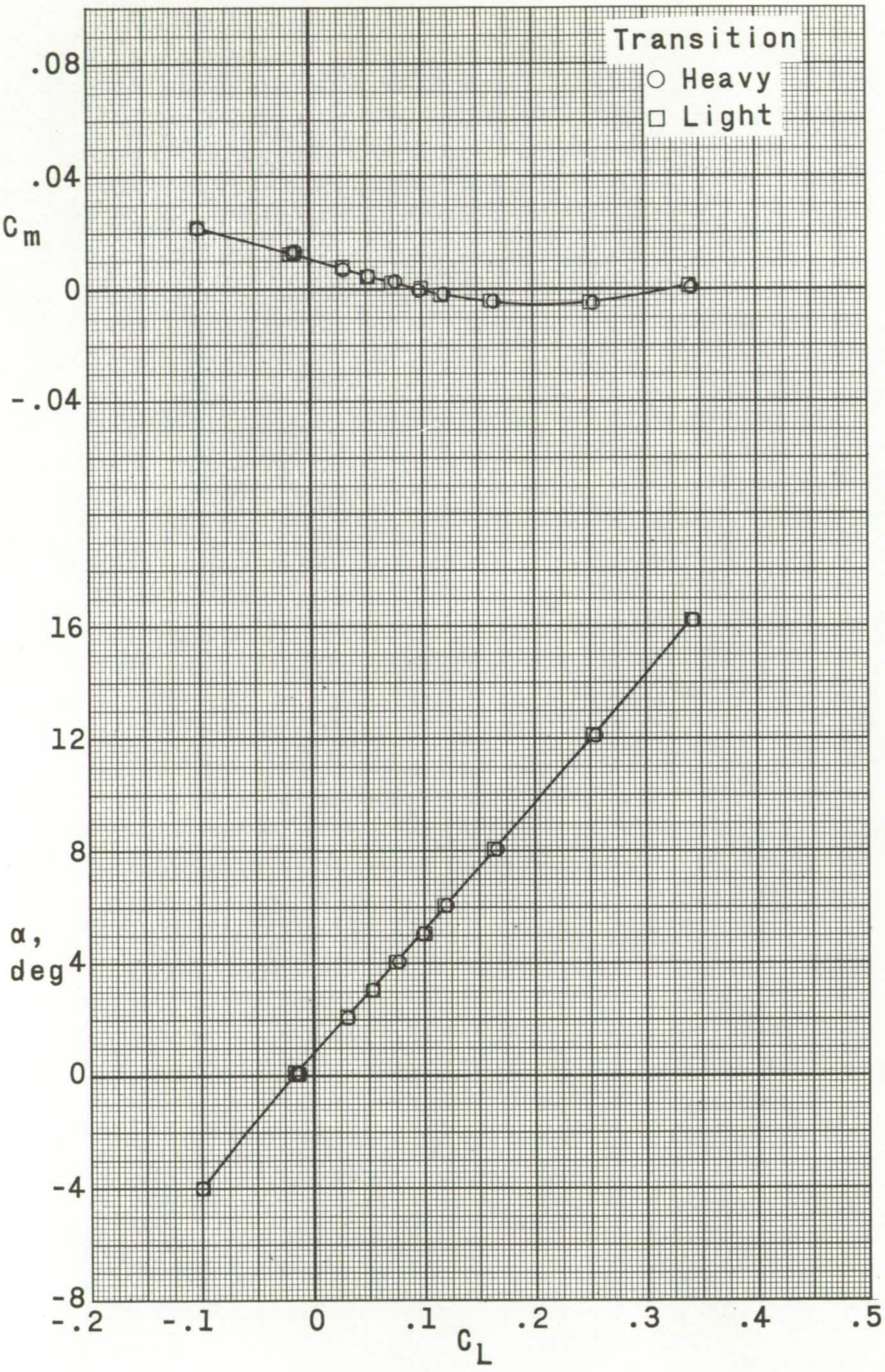

(c) M = 3.51.

Figure 7.- Continued.

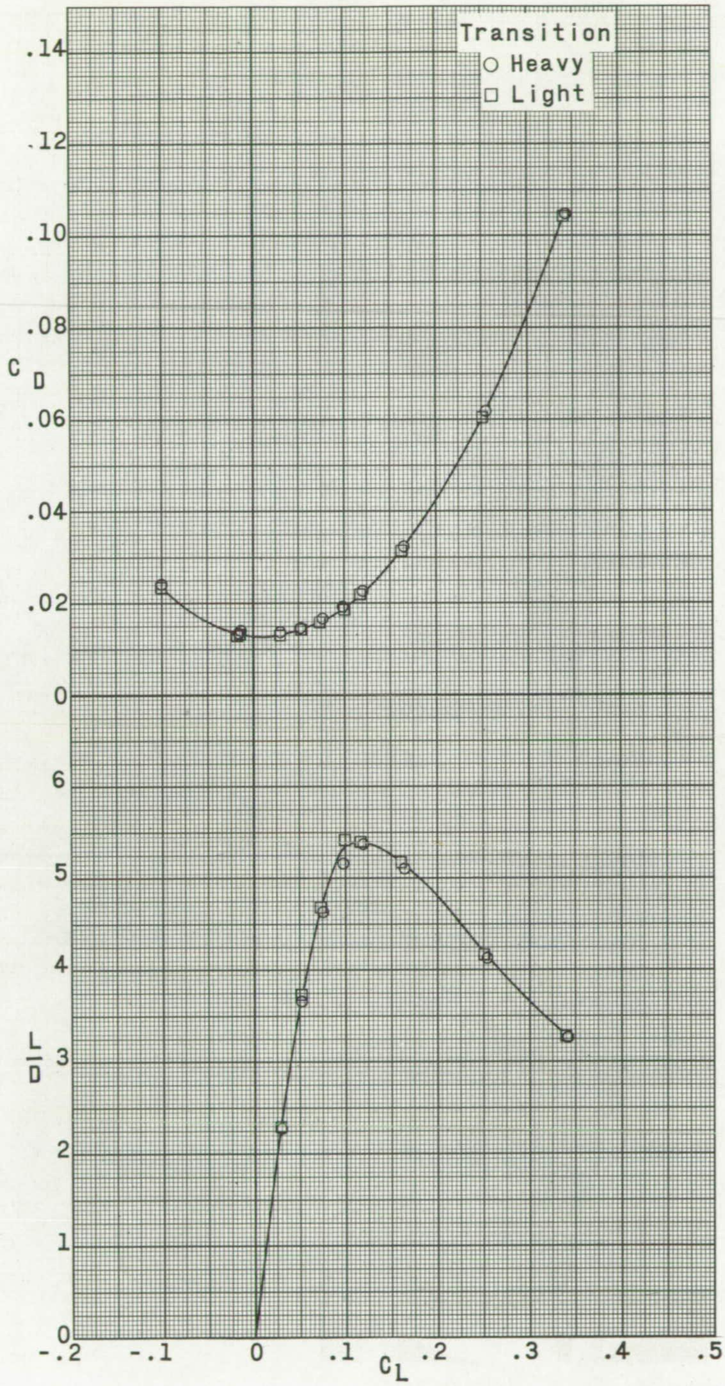

(c) Concluded.

Figure 7.- Concluded.

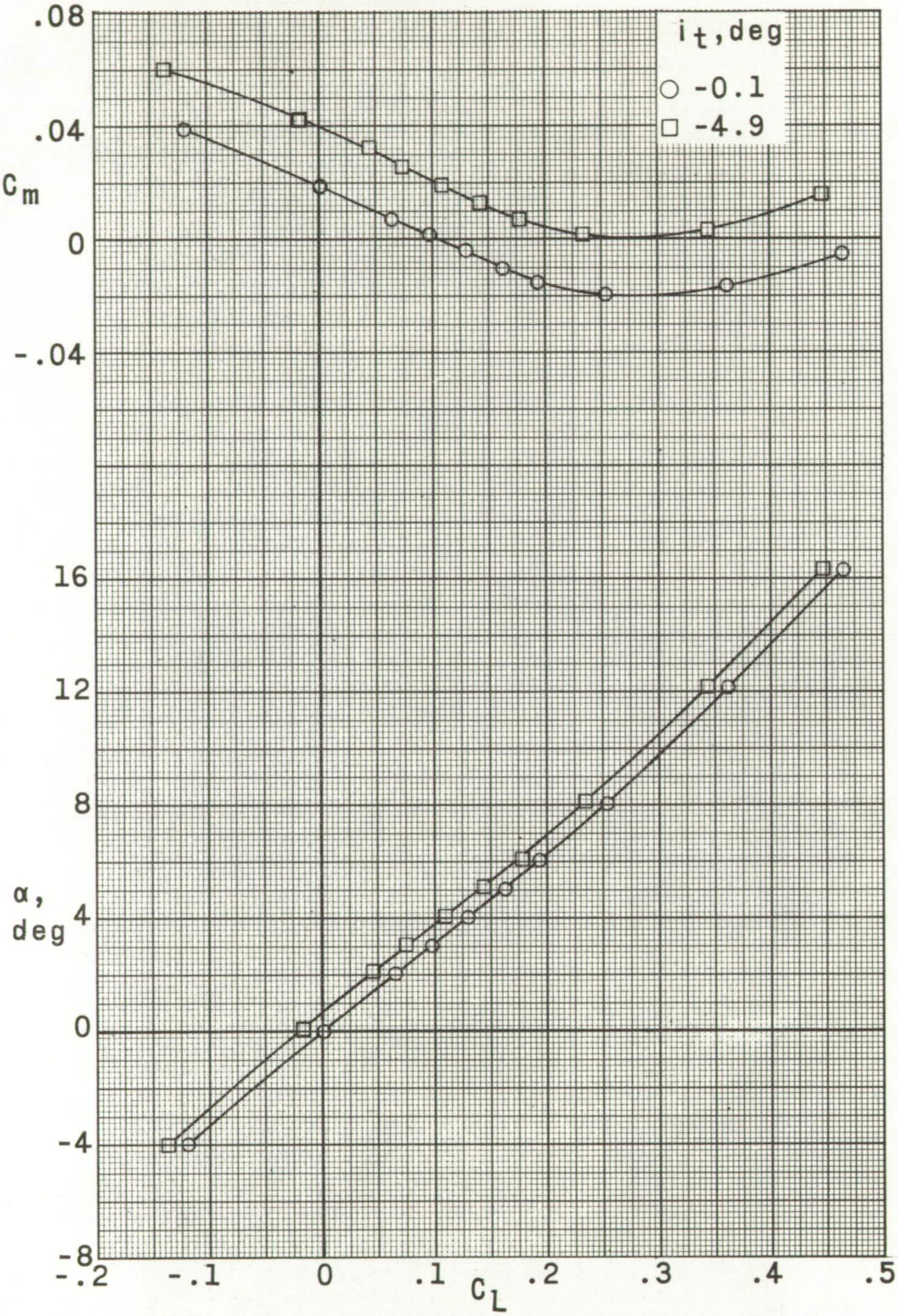

(a) M = 2.30.

Figure 8.- Effect of horizontal-tail incidence on aerodynamic characteristics in pitch of model with engine pack. $\theta_w = -2.8^\circ$; $\delta_v = \pm 1.5^\circ$; $\beta = 0^\circ$.

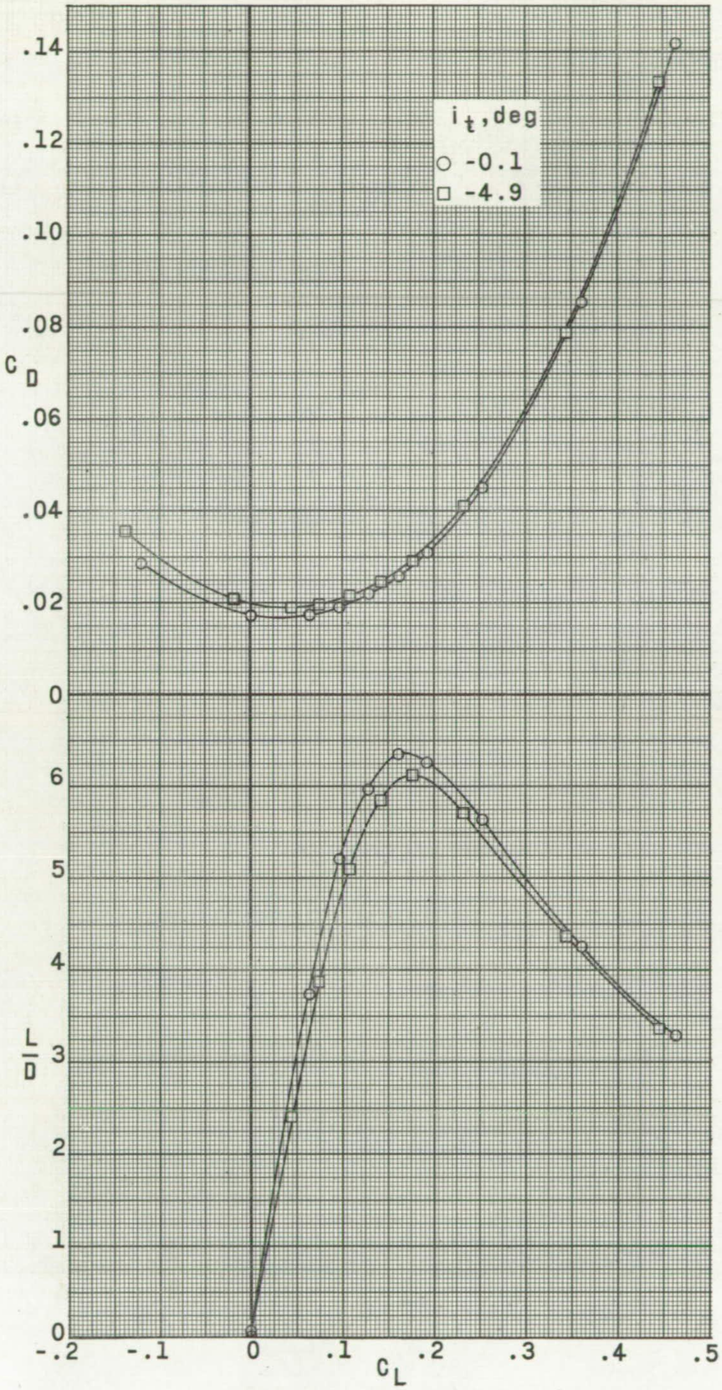

(a) Concluded.

Figure 8.- Continued.

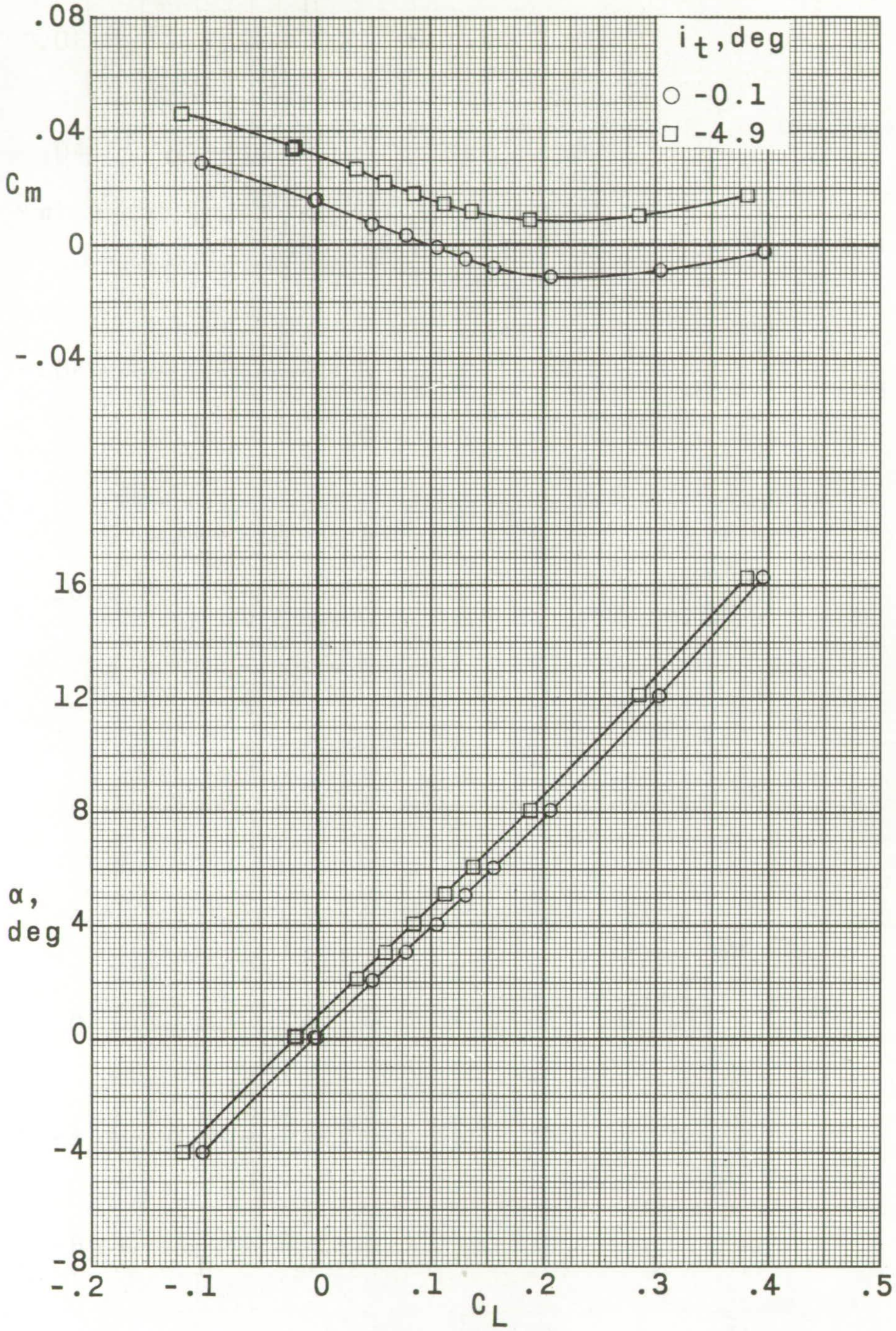

(b) M = 2.97.

Figure 8.- Continued.

[redacted]

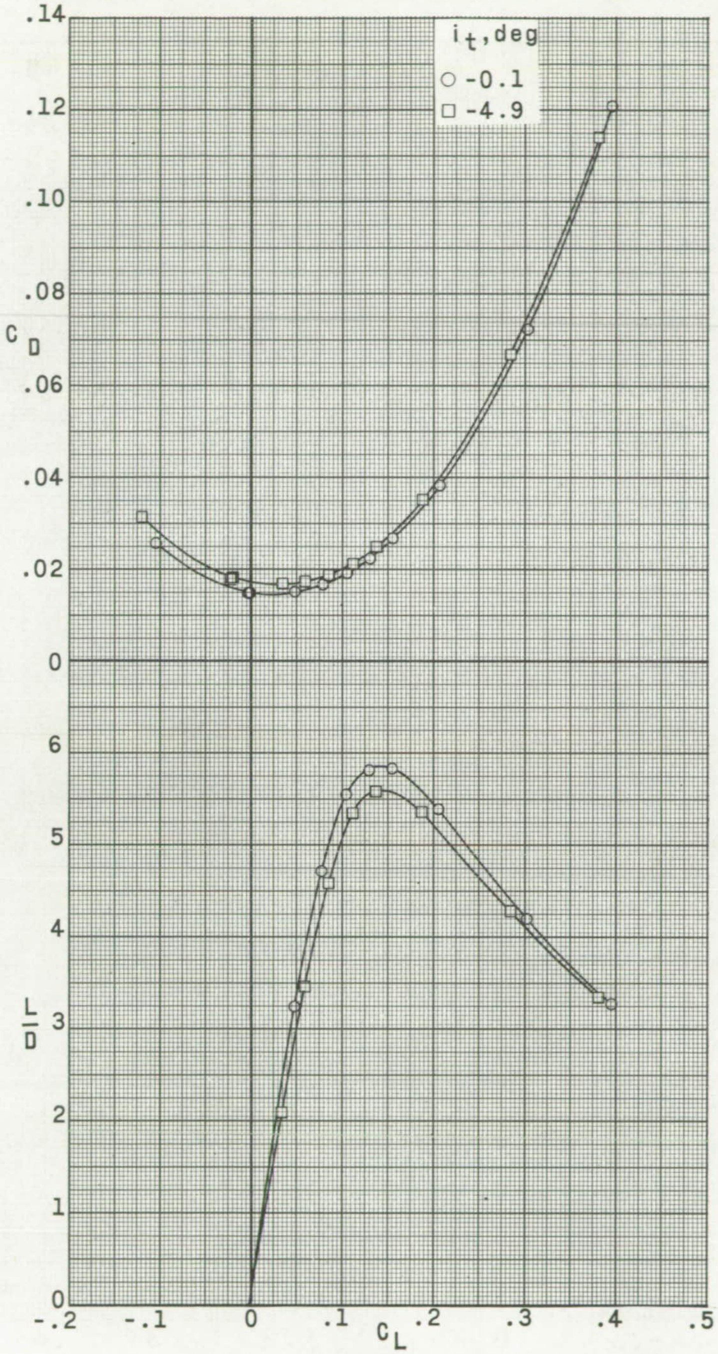

(b) Concluded.

Figure 8.- Continued.

[redacted]

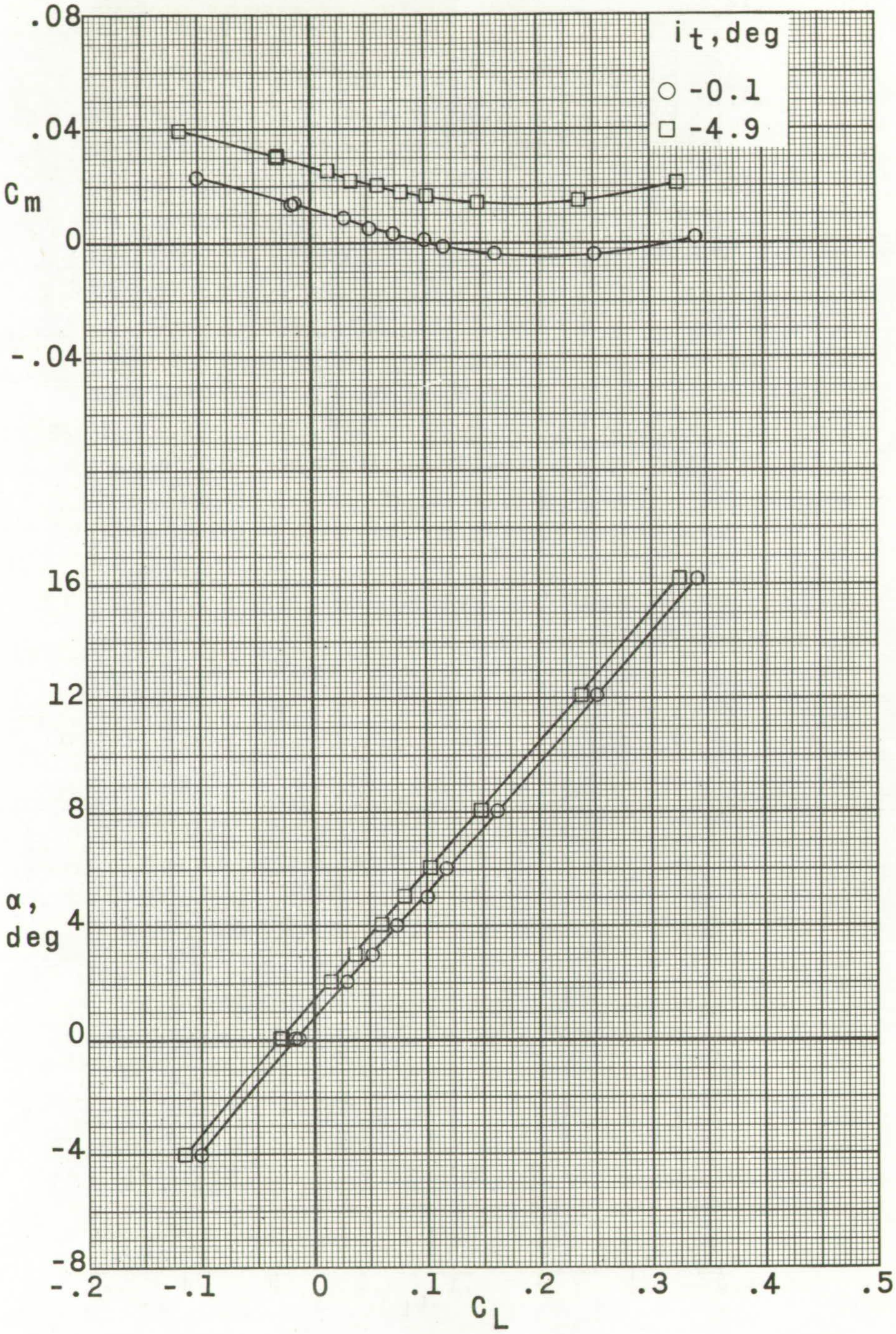

(c) M = 3.51.

Figure 8.- Continued.

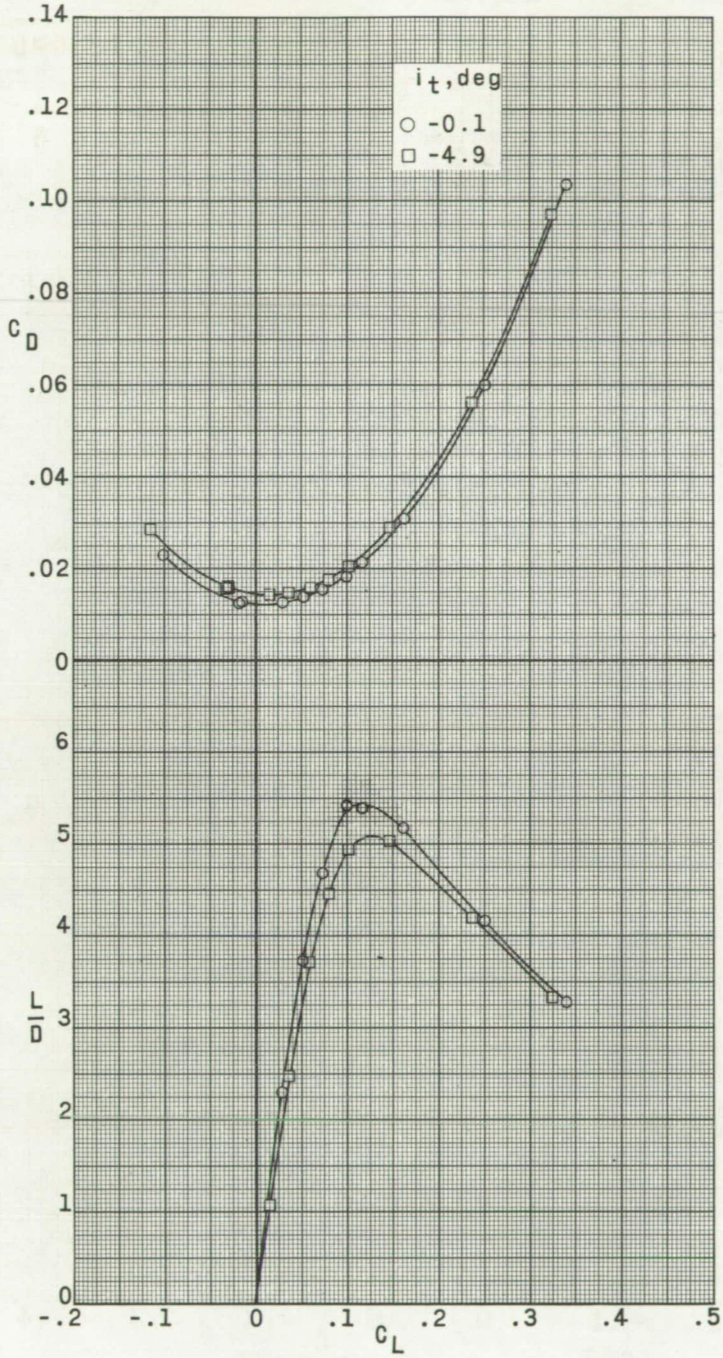

(c) Concluded.

Figure 8.- Concluded.

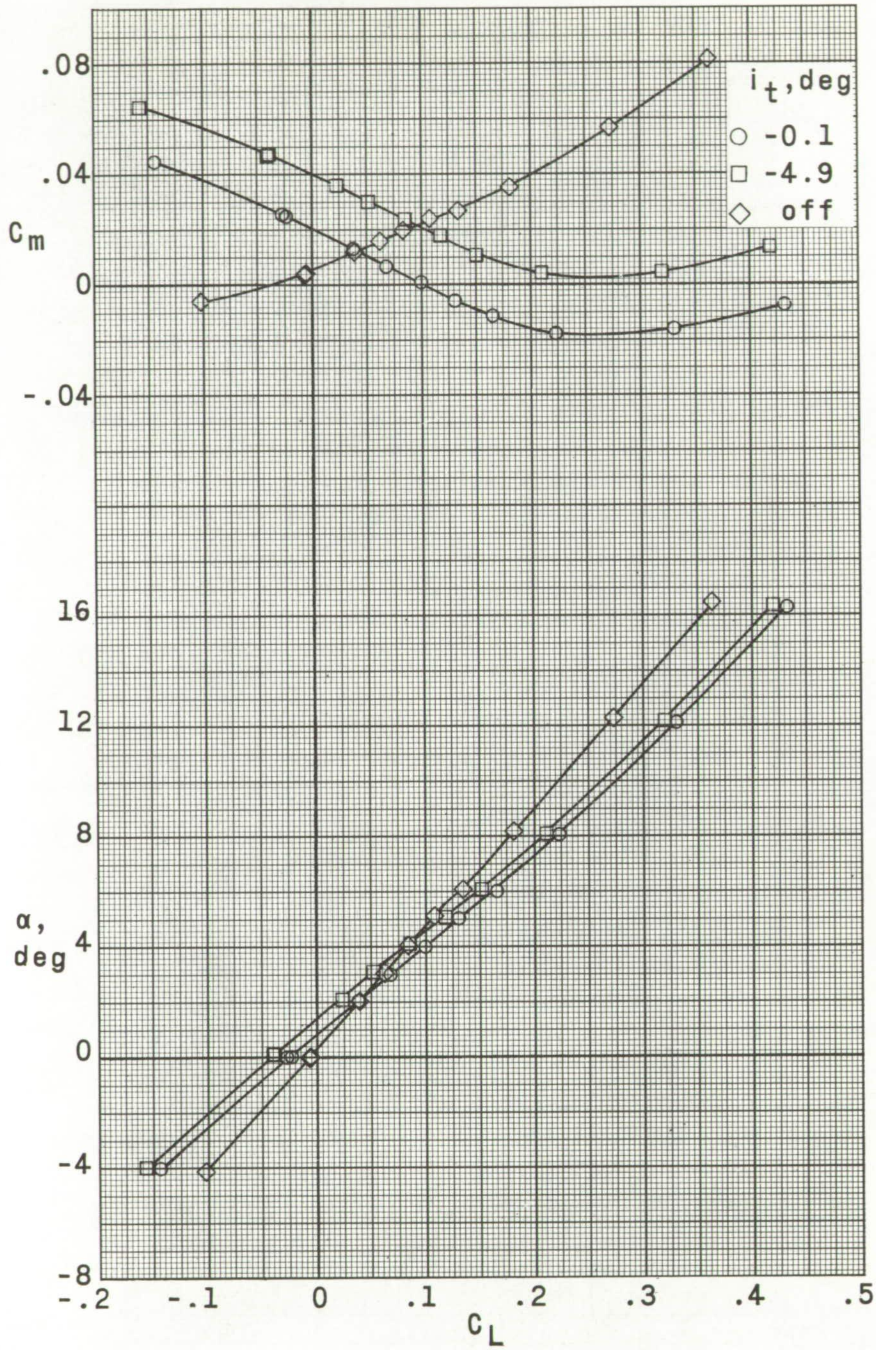

(a) M = 2.30.

Figure 9.- Effect of horizontal stabilizer on aerodynamic characteristics in pitch of model without engine pack. $\theta_w = -2.8^{\circ}$; $\delta_v = \pm 1.5^{\circ}$; $\beta = 0^{\circ}$.

DECLASSIFIED

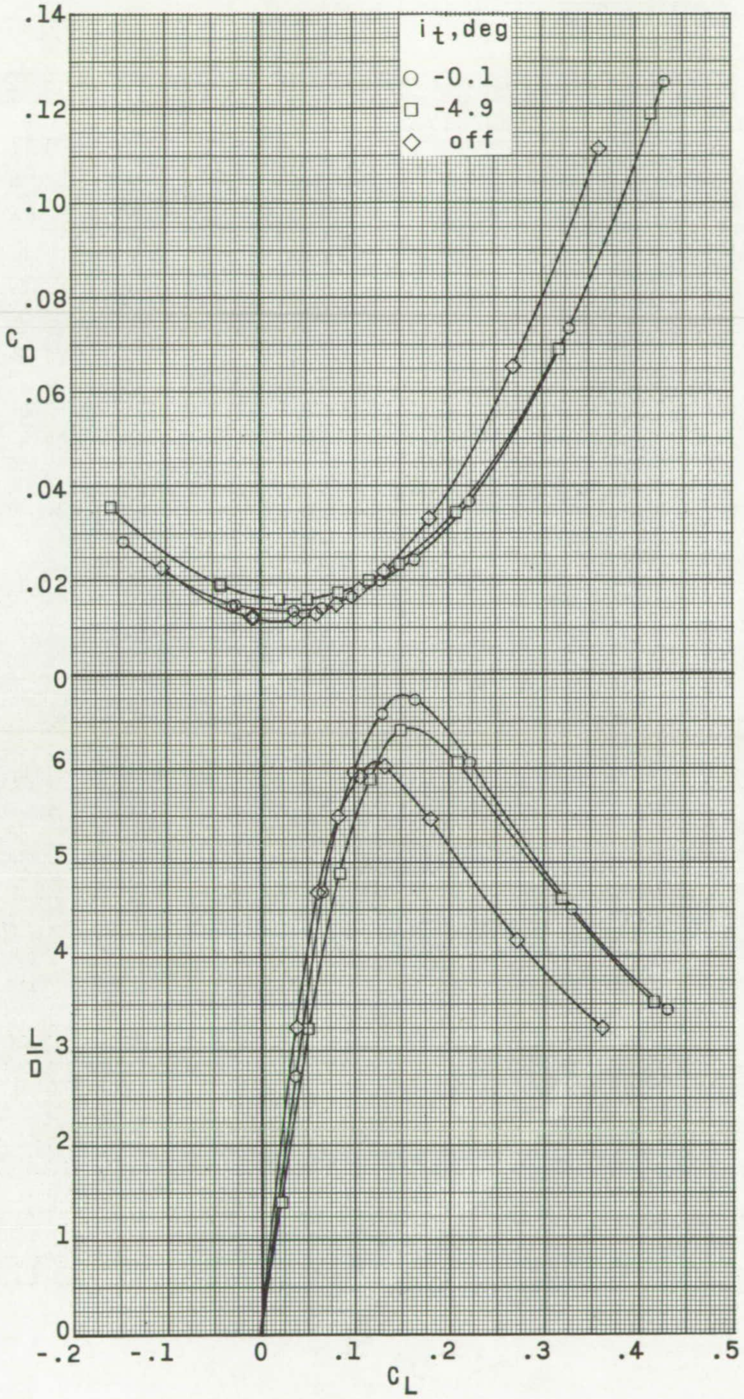

(a) Concluded.

Figure 9.- Continued.

[redacted]

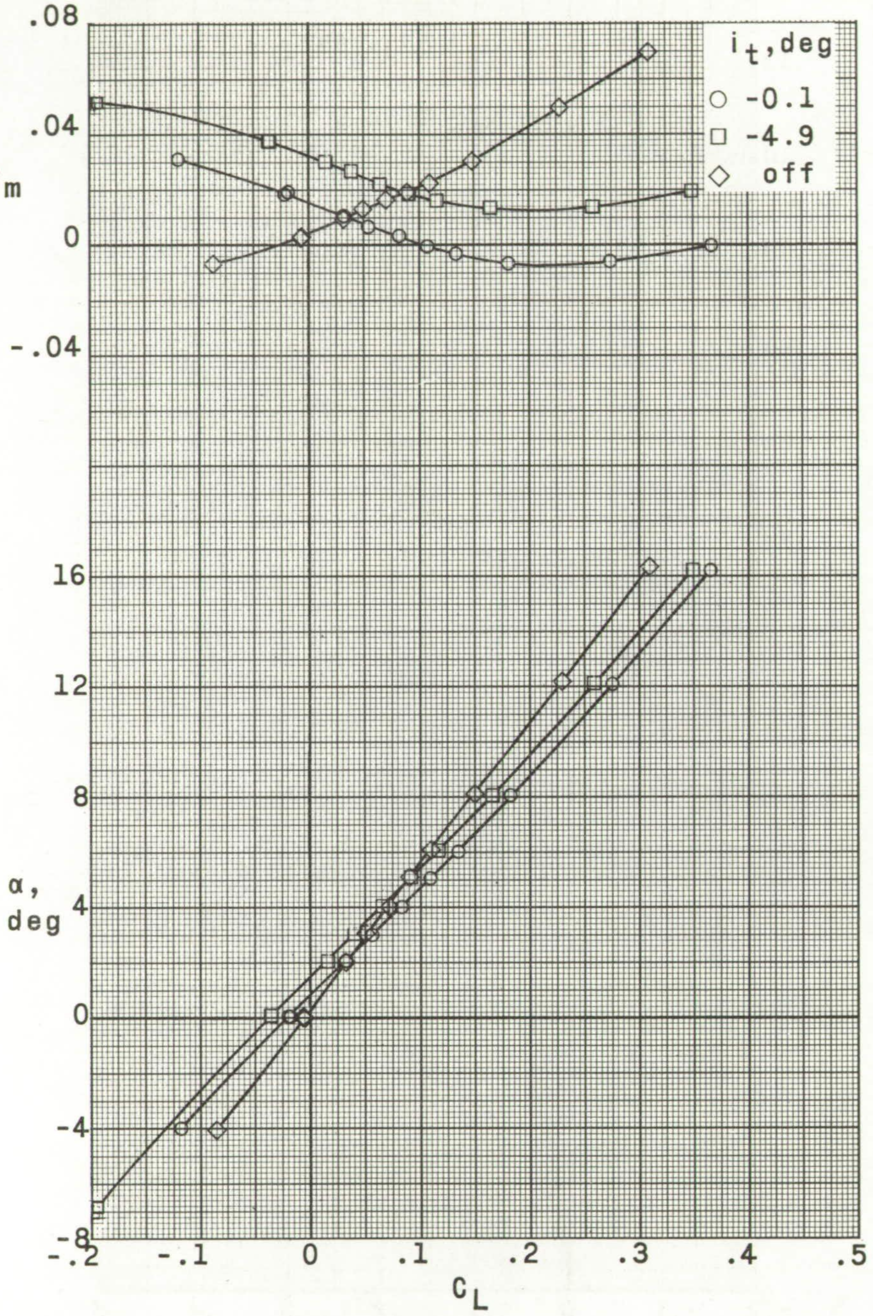

(b) M = 2.97.

Figure 9.- Continued.

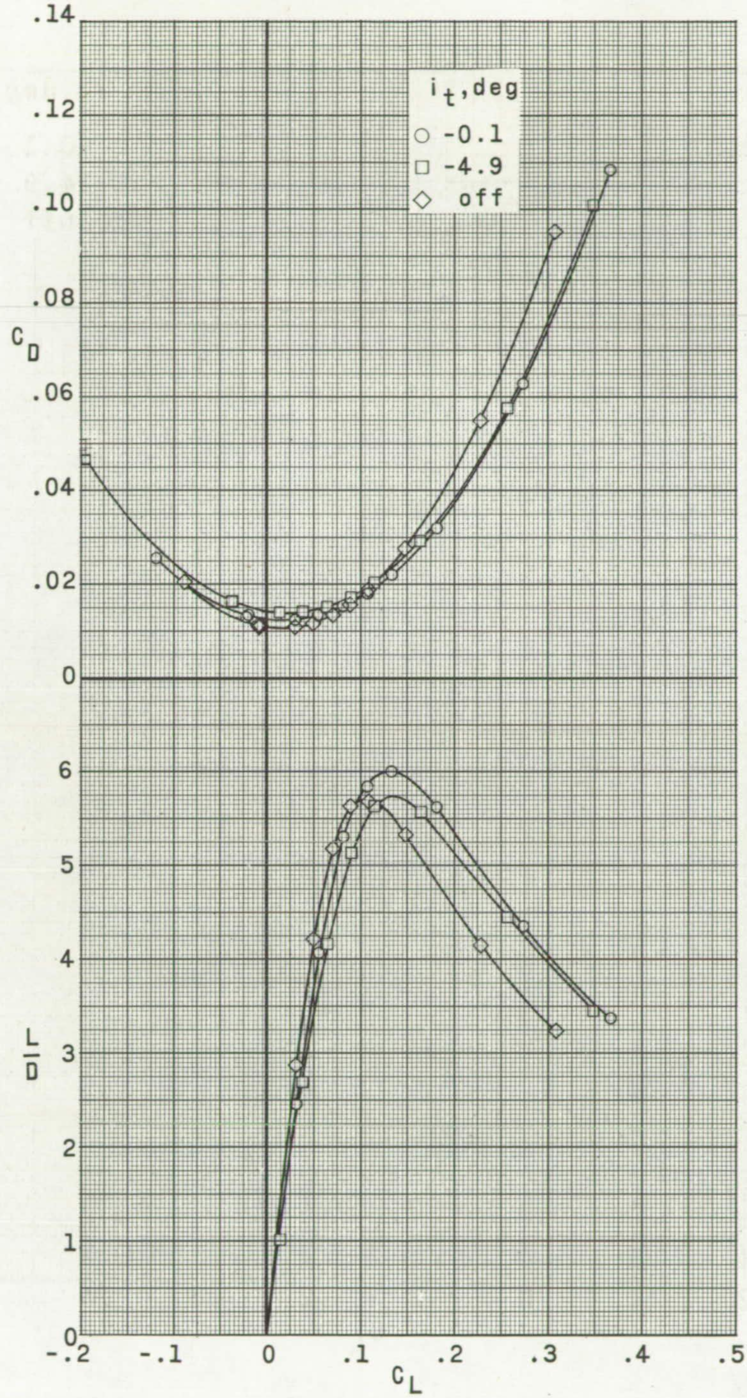

(b) Concluded.

Figure 9.- Continued.

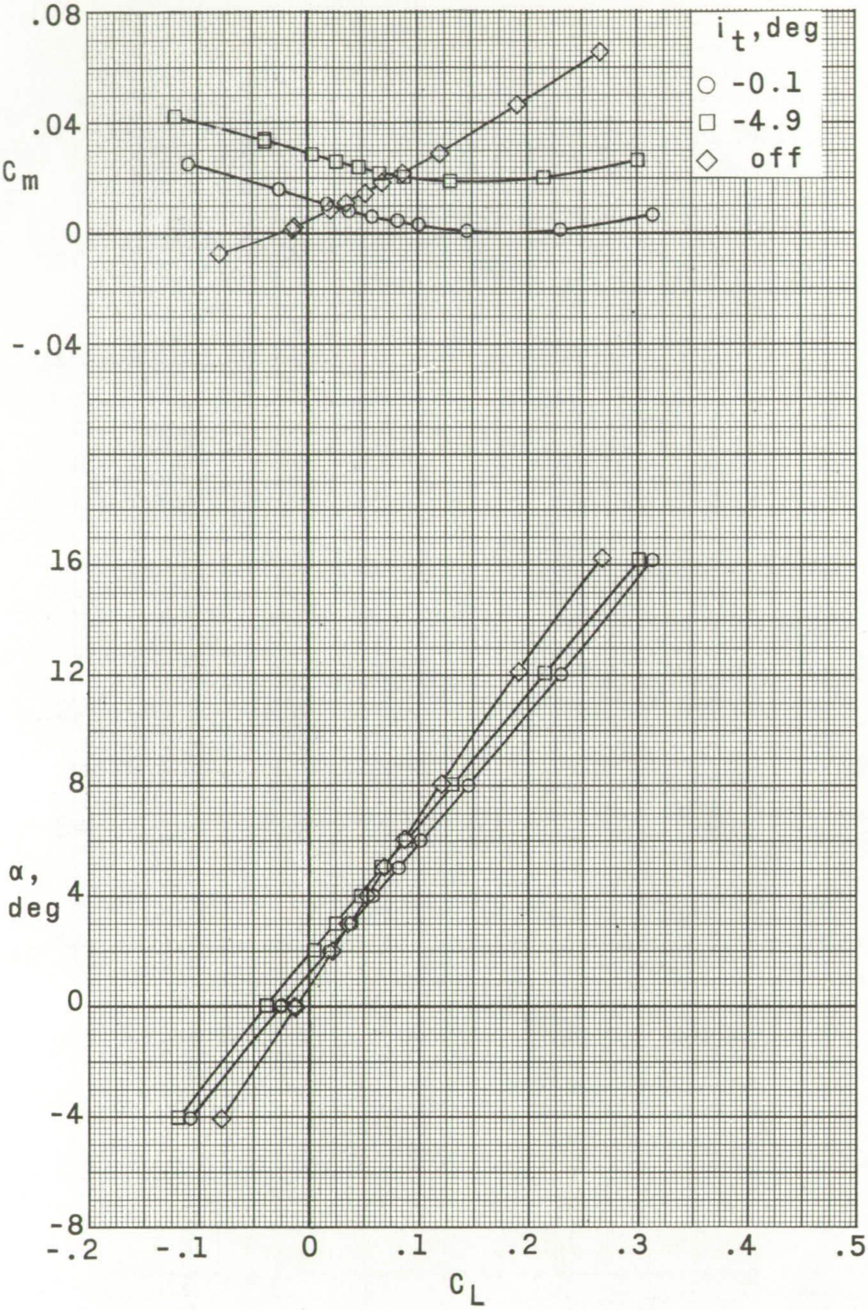

(c) M = 3.51.

Figure 9.- Continued.

[redacted]

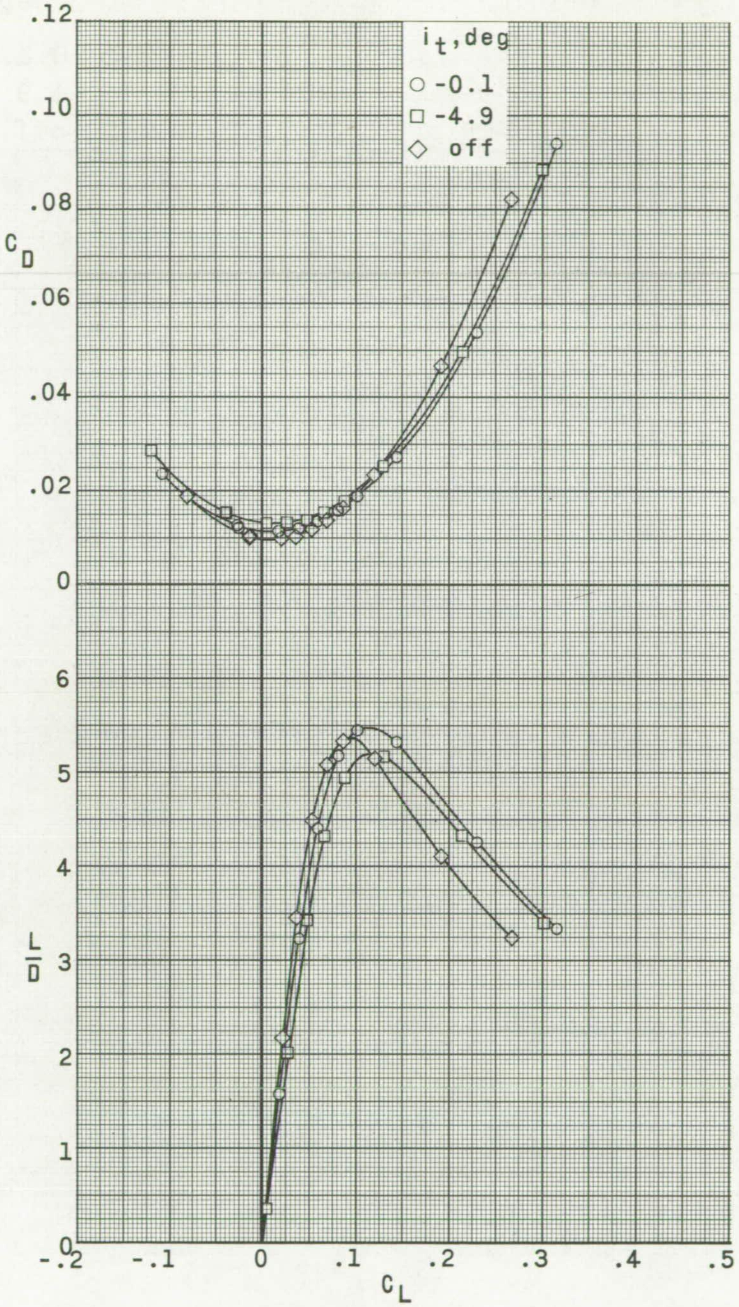

(c) Concluded.

Figure 9.- Concluded.

[redacted]

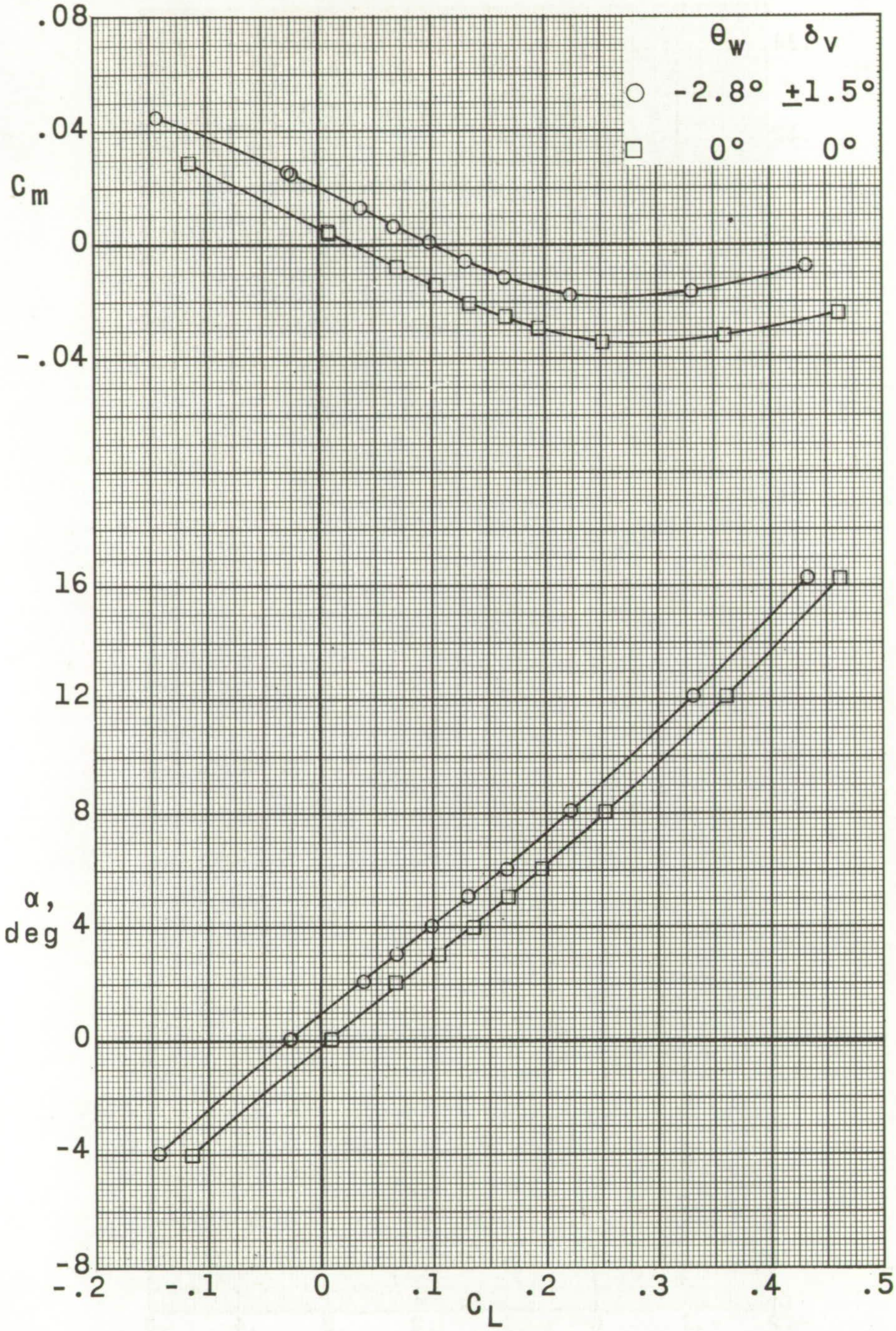

(a) M = 2.30.

Figure 10.- Effect of twist and toe on aerodynamic characteristics in pitch of model without engine pack. $i_t = -0.1^{\circ}$; $\beta = 0^{\circ}$.

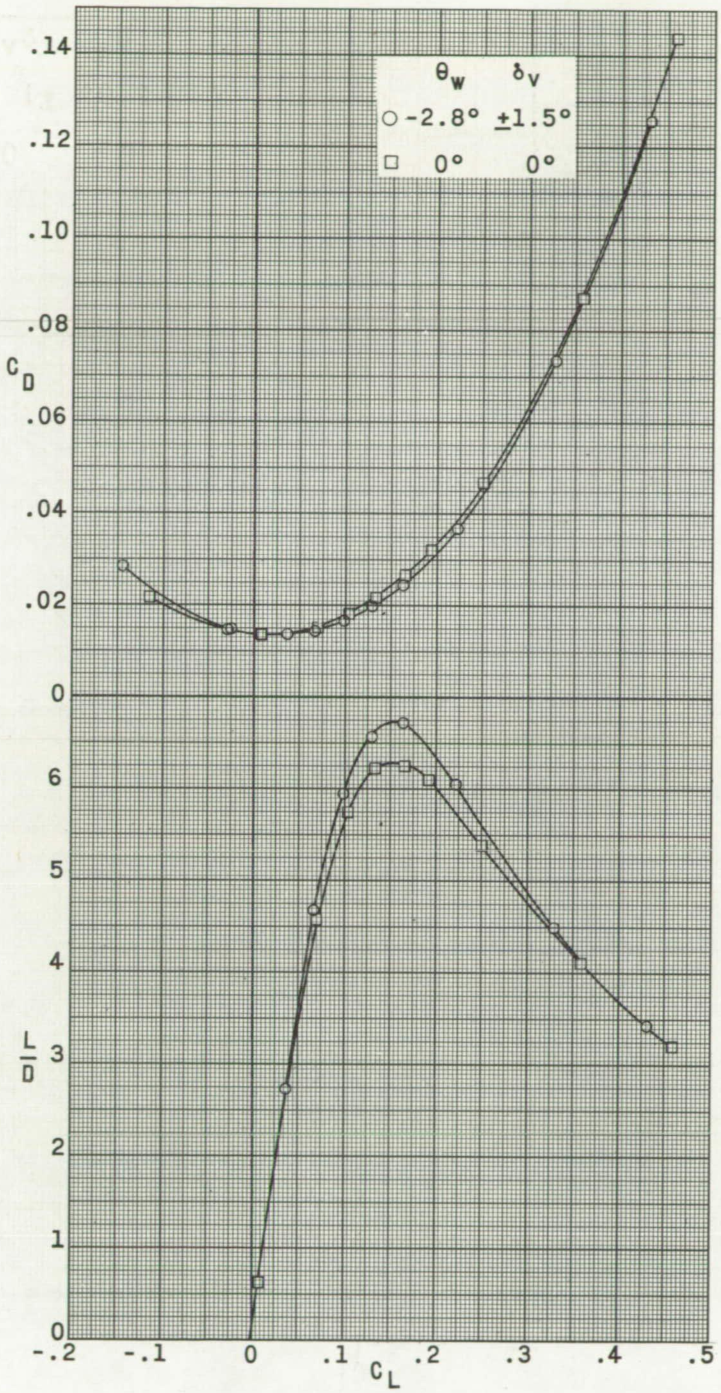

(a) Concluded.

Figure 10.- Continued.

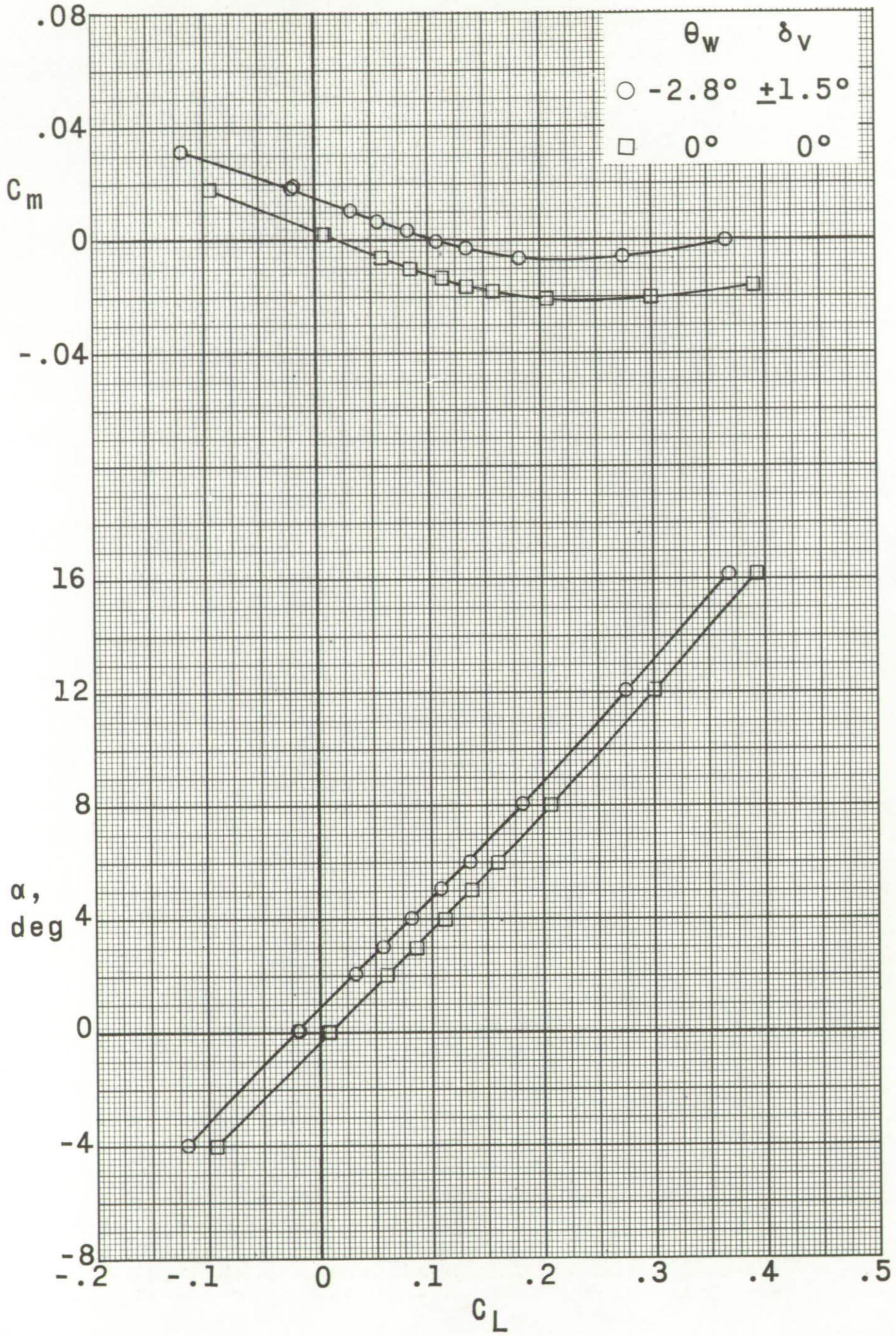

(b) M = 2.97.

Figure 10.- Continued.

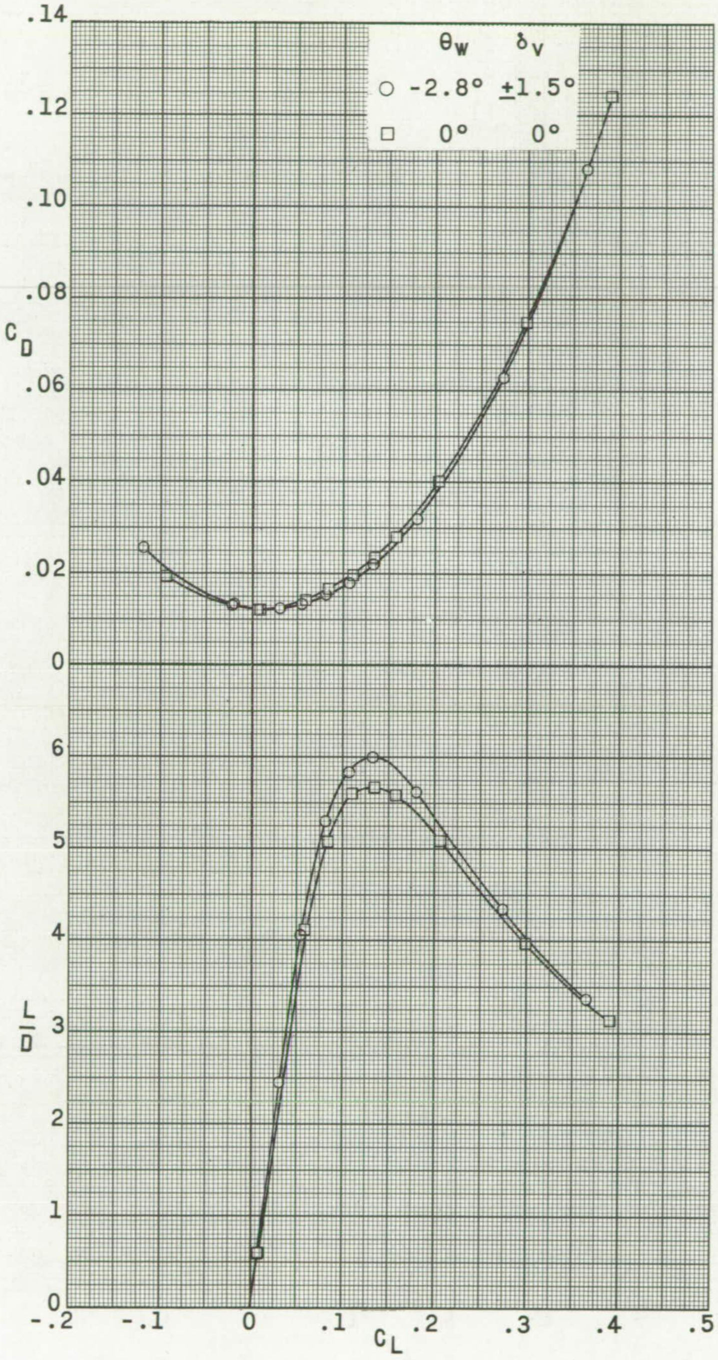

(b) Concluded.

Figure 10.- Continued.

[redacted]

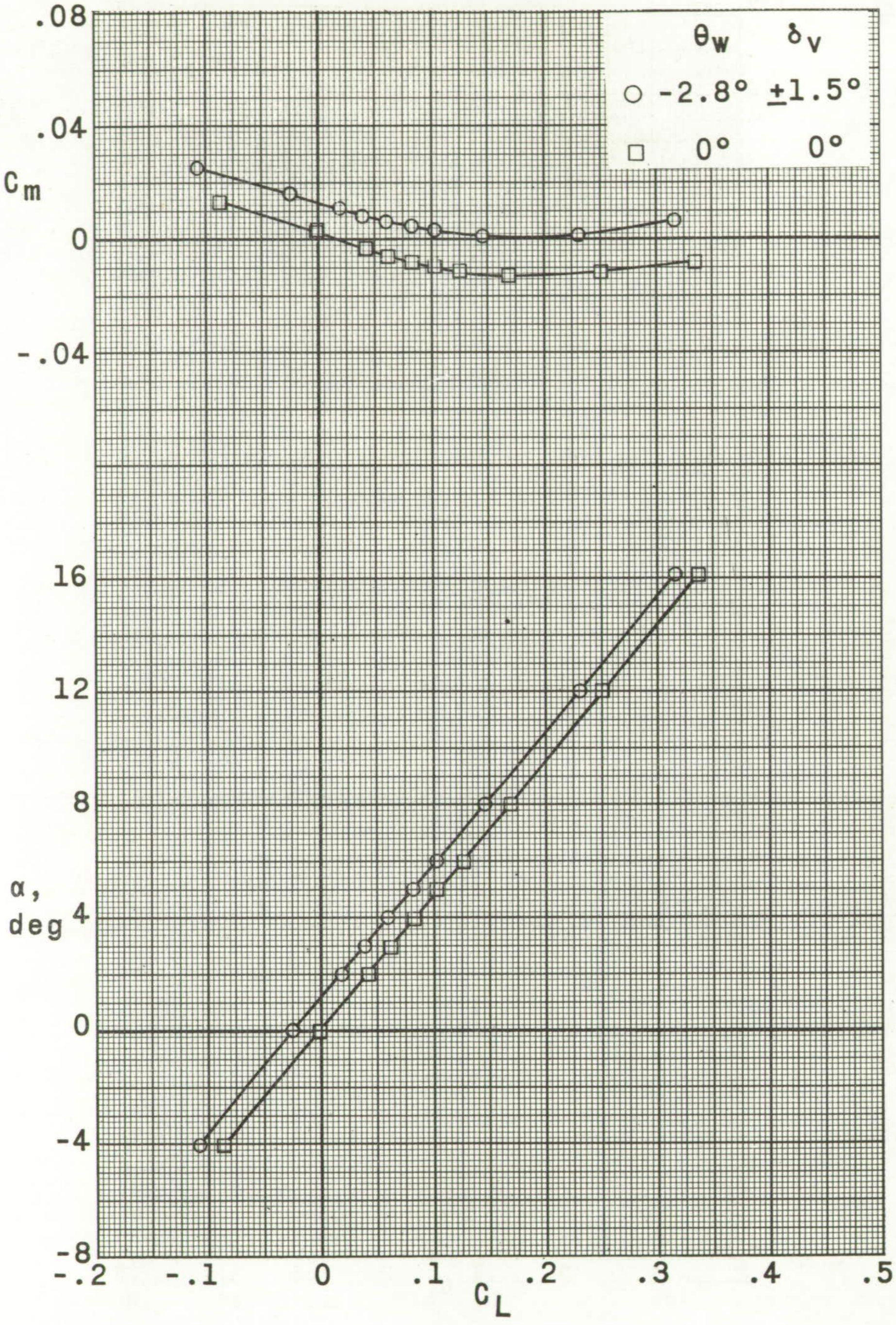

(c) M = 3.51.

Figure 10.- Continued.

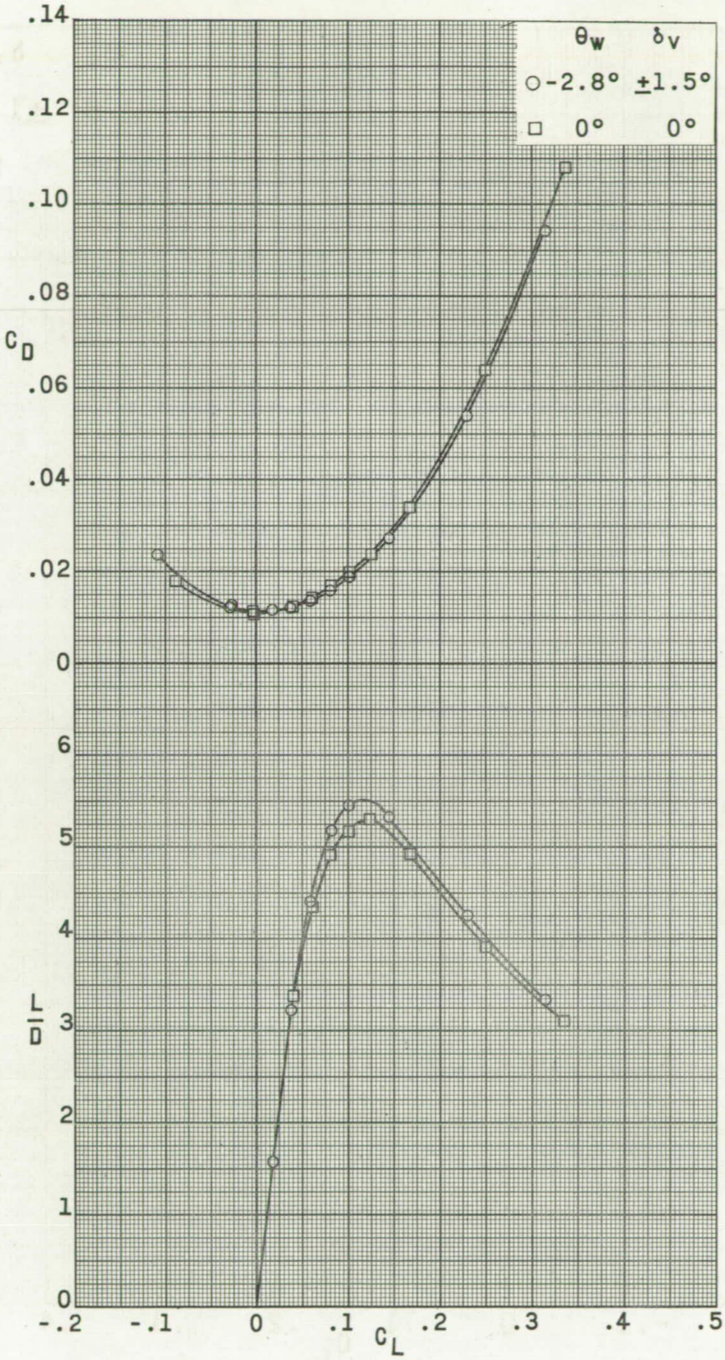

(c) Concluded

Figure 10.- Concluded.

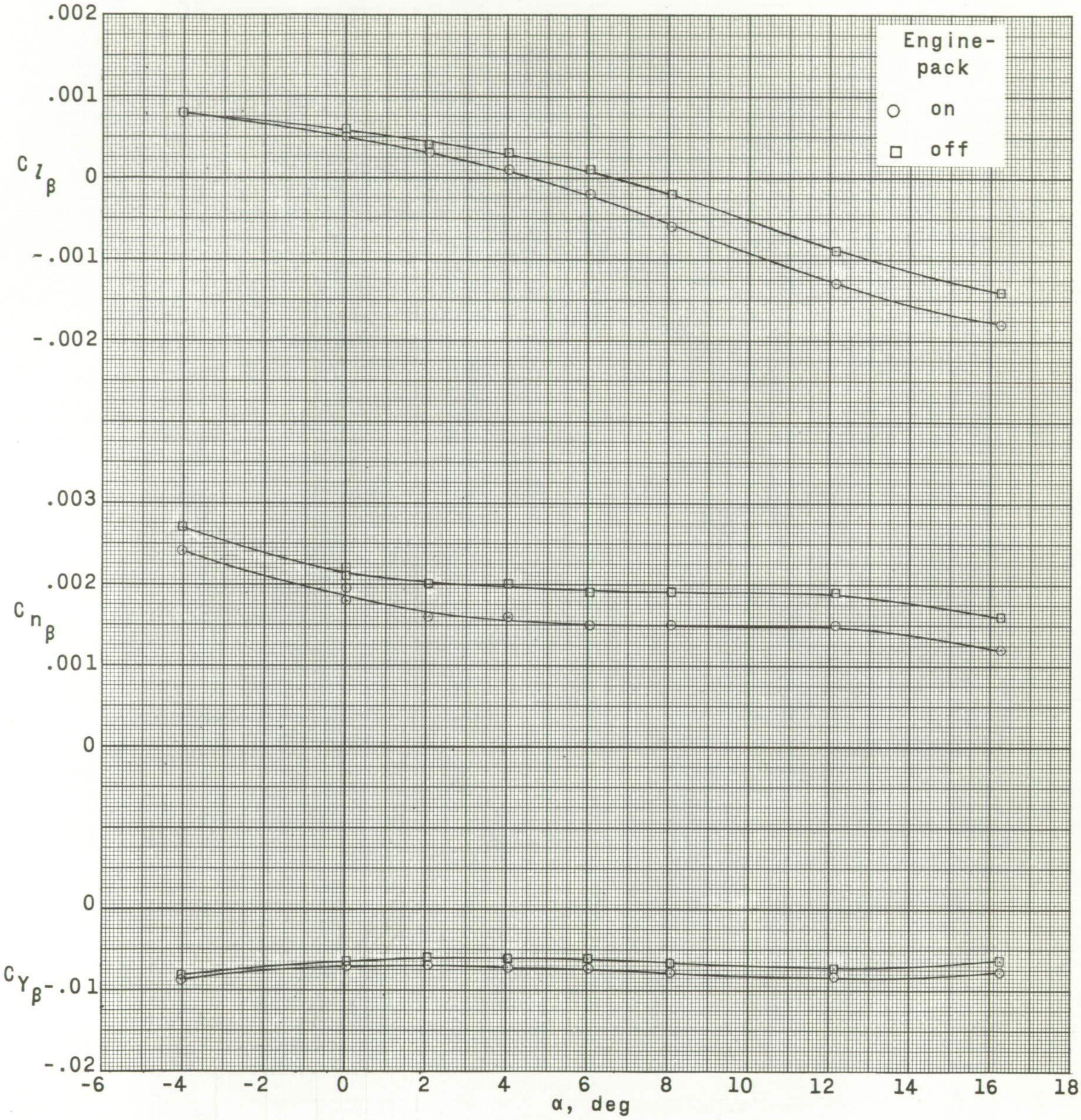

Figure 11.- Effect of engine pack on the variation of the static lateral-stability parameters with angle of attack. $M = 2.97$; $\theta_W = -2.8^\circ$; $\delta_V = \pm 1.5^\circ$; $i_t = -0.1^\circ$.

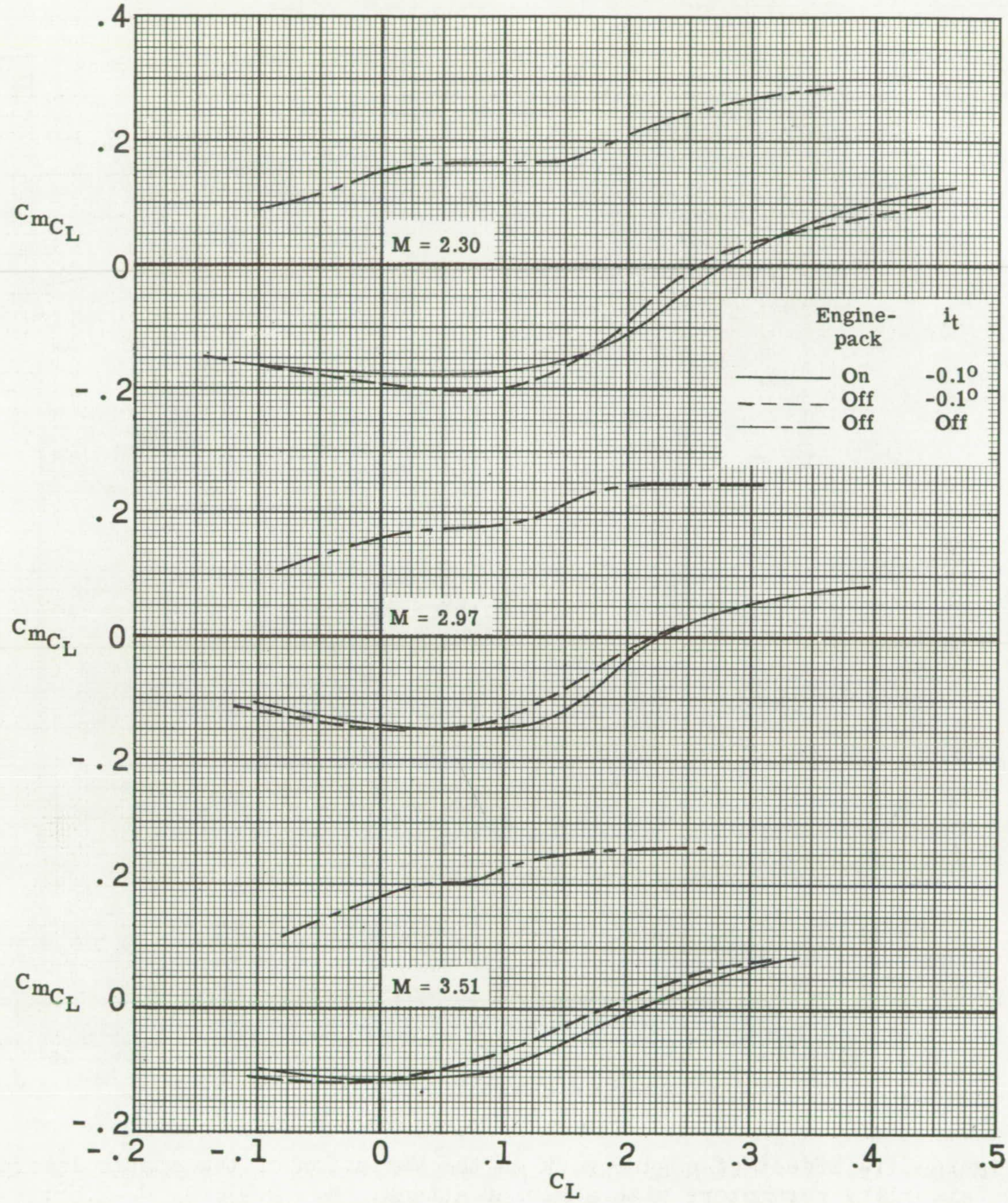

Figure 12.- Effect of engine pack and horizontal tail on the variation of the static longitudinal-stability parameter with lift coefficient. $\theta_w = -2.8^\circ$; $\delta_v = \pm1.5^\circ$; $\beta = 0^\circ$.

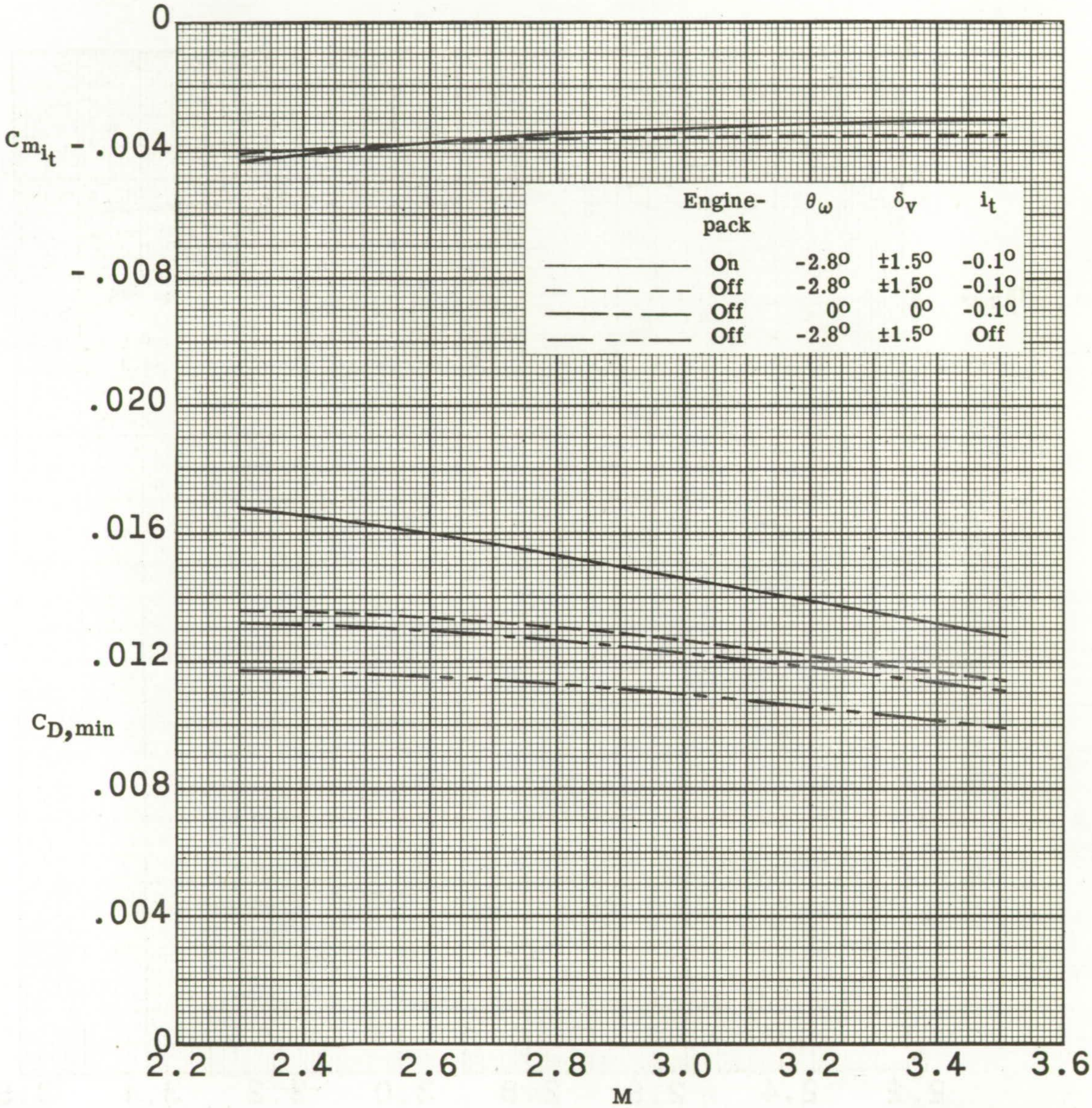

Figure 13.- Variation of stabilizer effectiveness and minimum drag coefficient with Mach number. $\beta = 0^{\circ}$.

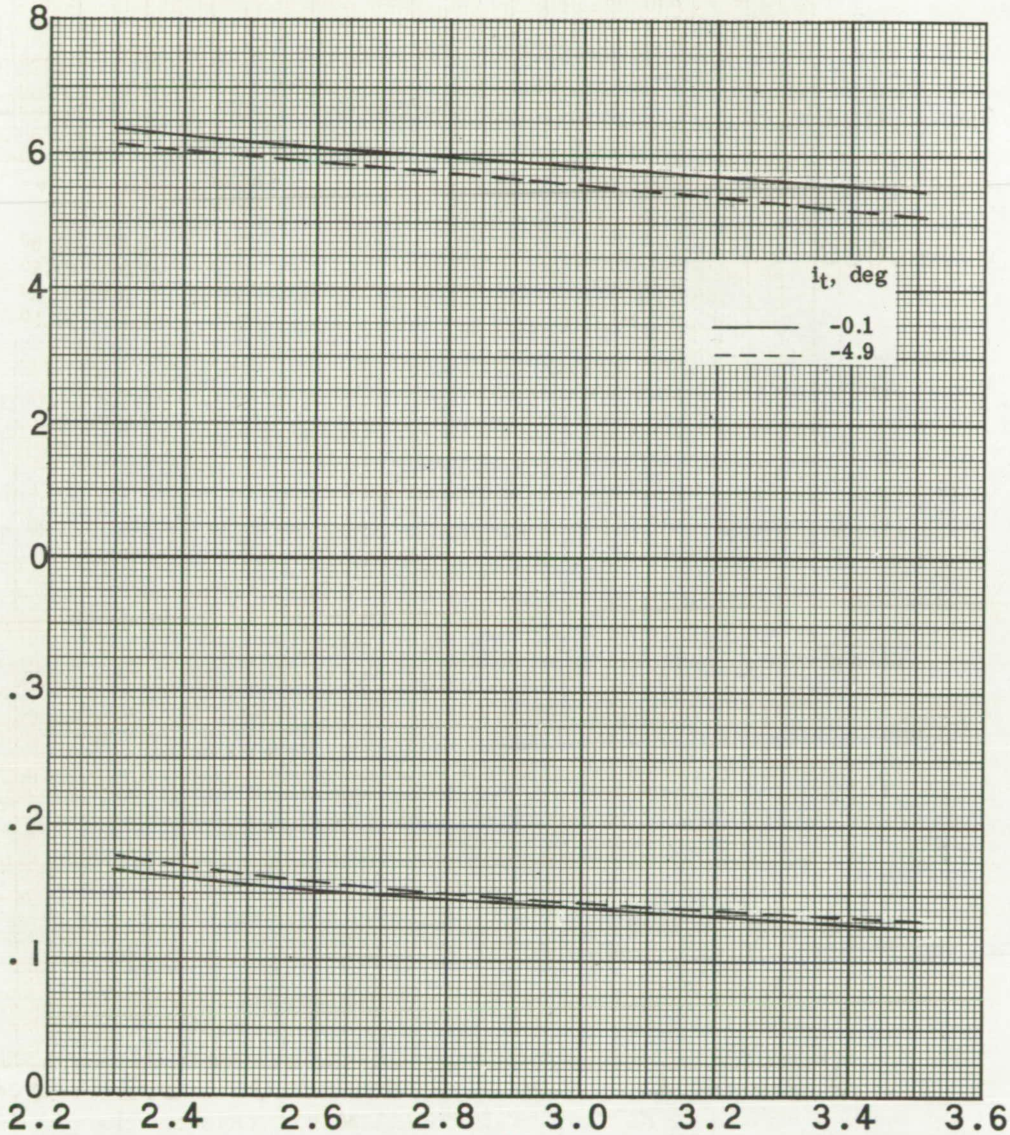

Figure 14.- Variation with Mach number of maximum lift-drag ratio and of lift coefficient for maximum lift-drag ratio. Model with engine pack; $\theta_W = -2.8^{\circ}$; $\delta_V = \pm 1.5^{\circ}$; $\beta = 0^{\circ}$.

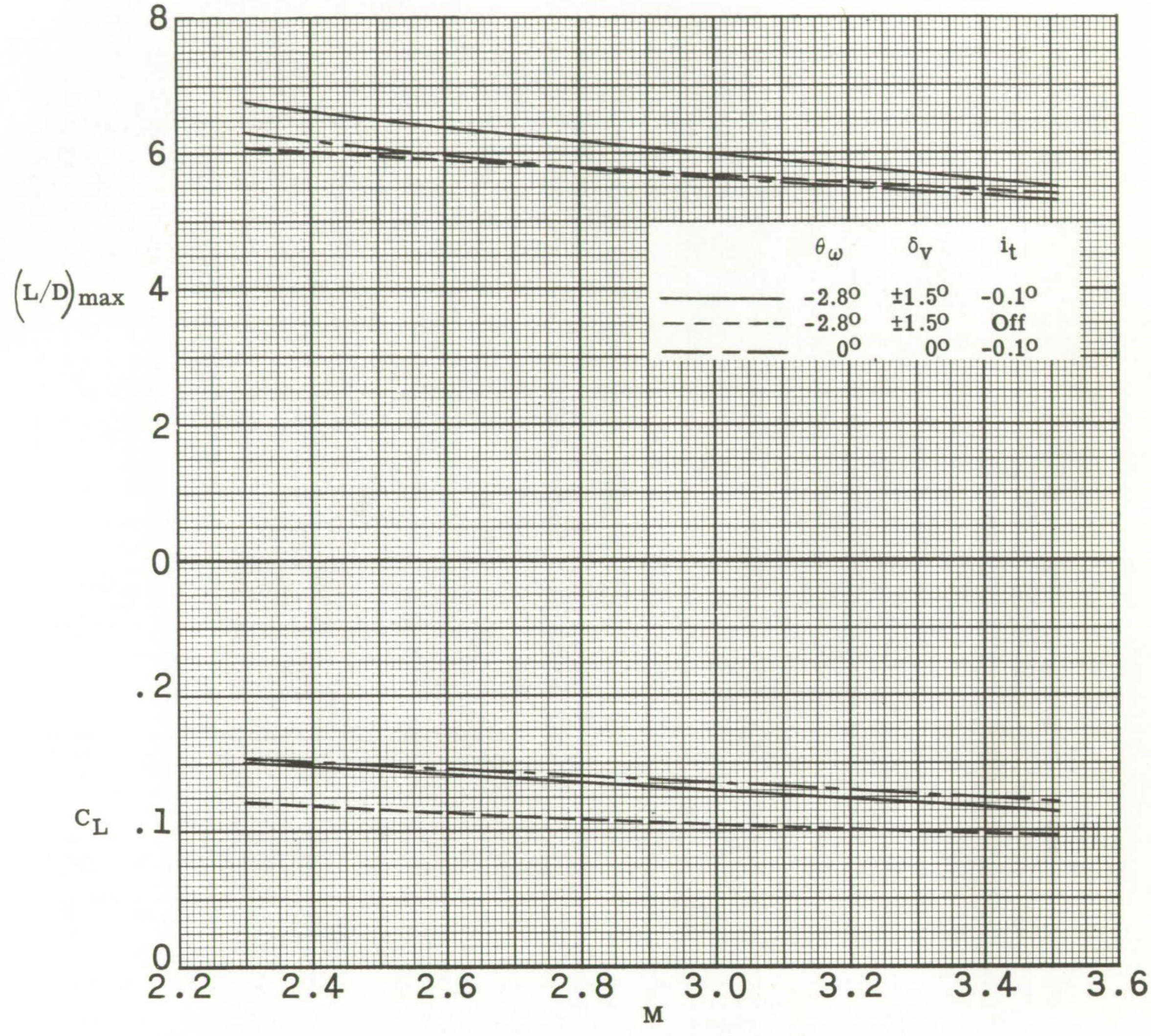

Figure 15.- Variation with Mach number of maximum lift-drag ratio and of lift coefficient for maximum lift-drag ratio. Model without engine pack; $\beta = 0^\circ$.

NACA - Langley Field, Va.

[redacted]

[redacted]